CATALYTIC OXIDATION OF METHANE IN A MICROCHANNEL REACTOR UNDER OXYGEN-LEAN CONDITIONS

by

İsmail Bahadır Kara

B.S., Chemical Engineering, Ege University, 2010

Submitted to the Institute for Graduate Studies in
Science and Engineering in partial fulfillment of
the requirements for the degree of
Master of Science

Graduate Program in Chemical Engineering
Boğaziçi University

2012

CATALYTIC OXIDATION OF METHANE IN A MICROCHANNEL REACTOR UNDER OXYGEN-LEAN CONDITIONS

APPROVED BY:

Assoc. Prof. Ahmet Kerim Avcı (Thesis Supervisor)	…….
Prof. Zeynep İlsen Önsan	…….
Assist. Prof. C. Can Aydıner	…….

DATE OF APPROVAL:

to my family

ACKNOWLEDGEMENTS

First of all, I would like to express my gratitude to my thesis supervisor Assoc. Prof. Ahmet Kerim Avcı. His advices and guidance always motivated me to improve my work. It was great honor to have the chance of practicing on his experiences in catalysis and reaction engineering.

I am very grateful to my thesis committee members; Prof. Zeynep İlsen Önsan and Assist. Prof. C. Can Aydıner.

I would like to thank Mustafa Karakaya, Eyüp Şimşek, Feyza Gökaliler and Melek Selcen Başar for their guidance and help during my thesis process. I also would like to express my gratitude to other members of CATREL team; Ali Uzun, Merve Eropak, İrem Şen, İpek Paksoy, Cansu Yassı.

Very special thanks goes to my friends Arda Arpak, Cihan Kaya and Hasan Yıldırım for their friendship. They always supported me through my master education.

Cordial thanks are for Bilgi Dedeoğlu, Nurettin Bektaş and Yakup Bal for their technical assistance and help during my thesis.

Finally, I would like to express my gratitude to my family for their endless support through my whole life. It is an honor for me to dedicate my thesis study to them.

Financial support for this study is provided by TÜBİTAK through project 108M509.

ABSTRACT

CATALYTIC OXIDATION OF METHANE IN A MICROCHANNEL REACTOR UNDER OXYGEN-LEAN CONDITIONS

The aim of this study is to investigate methane oxidation in a microchannel reactor under the effect of Pt, Rh and Ru catalysts supported on δ-Al_2O_3. Methane oxidation is an integrated part of the oxidative steam reforming (OSR) process which is based on coupling of exothermic oxidation and endothermic steam reforming of methane. As applied in OSR, experiments are conducted under fuel rich conditions that involved methane-to-oxygen (CH_4/O_2) ratios greater than the stoichiometric value of 0.50. In all experiments, amount of catalyst (Pt/δ-Al_2O_3, Rh/δ-Al_2O_3, Ru/δ-Al_2O_3) that is coated on a FeCrAl plate stayed in the range of 29 mg to 35 mg. The catalysts are prepared by the incipient-to-wetness impregnation method. Catalyst effect on methane conversion is determined according to two different experimental methods. In the first method four different inlet molar CH_4/O_2 ratios, 1.32, 1.59, 1.85 and 2.13, are applied at a constant total feed flow 100 ml/min by increasing reaction temperature from 623 K to 923 K for all three catalysts. The other method consisted of keeping CH_4/O_2 ratio at a constant value as 1.85 while changing feed flow stream to 75, 100 and 125 ml/min through increasing reaction temperature from 623 K to 923 K. Micro structural and elemental characterization of the fresh and used catalysts are achieved by scanning electron microscope (SEM) and energy dispersive X-ray spectroscopy (EDX) analyses. The catalysts performances are investigated in terms of CH_4 conversion. Methane conversion is found to increase with temperature regardless of the feed composition. Catalyst activity is found to follow the order of Pt/δ-Al_2O_3 > Rh/ δ-Al_2O_3 > Ru δ-Al_2O_3 with respect to their light-off temperature which is expressed as the value at which 10 per cent of methane conversion is achieved. For all catalysts, light-off temperatures are found to decrease and then increase with increasing values of CH_4/O_2 ratio. Higher methane conversion is achieved on Pt and Ru catalysts for increased contact time at CH_4/O_2 = 1.85. However Rh catalyst favors better conversion performance even at reduced contact time because of its high catalytic activity.

ÖZET

YALIN OKSİJEN ŞARTLARI ALTINDA MİKRO KANAL REAKTÖRDEKİ KATALİTİK METAN OKSİDASYONU

Bu çalışmanın amacı, δ-Al_2O_3 ile desteklenen Pt, Rh ve Ru katalizörleri etkisi altında, mikro kanal reaktörde metan oksidasyonunu araştırmaktır. Metan oksidasyonunun entegre olduğu oksijenli buhar reformlama (OSR) süreci, ekzotermik oksidasyon ve endotermik buhar reformlamanın birbirlerini ısıl olarak desteklemesine dayanır. Deneyler, OSR sürecinde olduğu gibi, stokiyometrik değerden (0.5) daha büyük molar metan/oksijen besleme oranı (CH_4/O_2) içeren zengin yakıt koşulları altında gerçekleştirilmektedir. Bütün deneylerde FeCrAl plakalarına kaplanan katalizör (Pt/δ-Al_2O_3, Rh/δ-Al_2O_3, Ru/δ-Al_2O_3) miktarları, 29 mg ile 35 mg arasında değişmektedir. Deneyler, 0.5 değerinden daha büyük molar metan/oksijen oranı (CH_4/O_2) içeren zengin yakıt koşulları altında gerçekleştirilmektedir. Katalizörler emdirme yöntemi ile hazırlanmıştır. Metan dönüşümündeki katalizör etkisi, iki farklı deneysel yönteme göre belirlenmiştir. Birinci yöntemde, üç katalizör için, reaksiyon sıcaklığı 623 K den 923 K e arttırılarak, 100 ml/dak sabit besleme akışında dört farklı molar CH_4/O_2 oranı (1.32, 1.59, 1.85 ve 2.13) uygulanılmıştır. Diğer yöntem ise reaksiyon sıcaklığı 623 K den 923 K e arttırılırken, CH_4/O_2 oranı (1.85) sabit bir değerde olarak, besleme akışını 75, 100 ve 125 ml/dak'ya değiştirmektir. Hazırlanan katalizörlerin yapısal ve temel tanımlamaları, taramalı elektron mikroskobu (SEM) ve enerji dağılımlı X-ışını spektroskopisi analiz yöntemleri ile yapılmıştır. Katalizörlerin performansları CH_4 dönüşümü açısından incelenmiştir. Metan dönüşümünün, girdi bileşiminden bağımsız olarak, sıcaklık ile arttığı tespit edilmiştir. Katalizörlerin aktivitesi, metan dönüşümünün 10% olduğu sıcaklık temel alınarak incelendiğinde, Pt/δ-Al_2O_3 > Rh/δ-Al_2O_3 > Ru/δ-Al_2O_3 sıralamasını takiben azalmıştır. Bütün katalizörlerde, %10 dönüşümünün elde edildiği sıcaklık değeri, artan CH_4/O_2 oranı ile önce azılmış, sonra artma eğilimi göstermiştir. Pt ve Ru katalizörleri üzerinde temas süresi arttırıldığında, CH_4/O_2 = 1.85 oranında, daha yüksek metan dönüşümleri elde edildiği görülmüştür. Ancak Rh katalizörü, yüksek katalitik aktivitesi sayesinde, düşük temas süresinde bile daha iyi dönüşüm performansını desteklemektedir.

TABLE OF CONTENTS

LIST OF FIGURES

LIST OF TABLES

LIST OF SYMBOLS

ΔH^0_{298}	Standard Enthalpy of Formation
K	Degree
^oC	Degree
wt%	Weight Percent
g_{cat}	Gram Catalyst

LIST OF ACRONYMS/ABBREVIATIONS

CPO	Catalytic Partial Oxidation
EDX	Energy Dispersive X-ray Spectroscopy
EU5	Euro 5
EU6	Euro 6
GC	Gas Chromatograph
ID	Inside Diameter
NASA	National Aeronautics and Space Administration
OSR	Oxidative Steam Reforming
PO	Partial Oxidation
SEM	Scanning Electron Microscope
SR	Steam Reforming
TCD	Thermal Conductivity Detector
WGS	Water-Gas Shift Reaction

1. INTRODUCTION

The huge world reserve of natural gas, which is essentially methane (CH_4), appears as an attractive source of energy for heat and power production, and propulsion. The low amounts of sulphur and nitrogen containing constituents in natural gas are beneficial and give low emission levels of sulphur and nitrogen oxides (SO_x and NO_x) during combustion. For efficient and environmentally sustainable conversion of methane, catalytic combustion offers an attractive alternative to conventional combustion, since the energy is released at moderate temperatures and the emission levels of carbon monoxide and nitrogen oxides are relatively low. Since methane is a greenhouse gas, such processes demand controlled methane handling with low methane slip.

In addition to its use for energy generation, methane oxidation is an integrated part of the oxidative steam reforming (OSR) process used to produce a hydrogen-rich mixture that can be used either in fuel cells (after CO clean-up) or as synthesis gas ($CO+H_2$) in Fisher-Tropsch or methanol syntheses. Methane OSR is based on the coupling of exothermic oxidation and endothermic steam reforming of methane. Rate of heat transfer between these reactions, which depends on the reactor type, dictates the efficiency of OSR. At this point, use of microchannel reactors involving wall-coated catalysts appears as a promising option due to their inherently improved transport rates.

This study aims the investigation of methane oxidation in a microchannel reactor, in which the catalysts will be integrated as a thin layer into the inner channel wall. The reaction will be studied under the fuel-rich conditions typically applied in the OSR process. Several catalysts such as Pt, Rh and Ru are tested at different molar methane-to-oxygen ratios and at different flow rates with constant methane-to-oxygen ratio at the reactor inlet for their oxidation activities.

2. LITERATURE SURVEY

2.1. Catalytic Methane Oxidation

Catalytic combustion has very attractive characteristics compared with flame combustion. The combustion temperature is lower and combustion is performed at a concentration range outside of flammability limits, due to the complete oxidation property. As a result, almost no NO_x, CO or particulate matter can be observed (Guan *et al.*, 2008).

Catalytic combustion is one means of meeting increasingly strict emissions requirements for industrial and utility gas turbines. Natural gas, which is composed mainly of methane, has recently attracted attention because it combusts with less byproducts compared to other fuels (Guan *et al.*, 2008). Natural gas is currently the fuel of choice for power-generating gas turbines, and therefore catalytic combustion of methane has been the focus of interest in recent years. By enabling stable low-temperature combustion (as low as 1200 °C), NO_x emissions from natural-gas-fueled catalytic combustors can be below 3 ppm, with single-digit CO/UHC emissions and with low levels of combustor acoustic noise (Lyubovsky *et al.*, 2003).

Furthermore CH_4 (which is the main component of natural gas exhausts) has the highest hydrogen content, which allows achieving a reduction of CO_2 per MJ emissions with respect to other hydrocarbon fuels. However, the abatement of unburned methane, which constitutes about 90% by volume of natural gas, still remains a demanding challenge in view of the 100mg/km limit introduced in EU5/EU6 regulations for total hydrocarbon (THC), since the methane molecule is very stable and requires high temperatures to be oxidized **(**Bounechada *et al.*, 2012).

It has been well recognized over the years that it would be highly desirable both economically and environmentally to be able to lower the threshold temperature of the oxidation reactions of common gaseous-fuels in air and burn fuel–air mixtures that are leaner

than their recognized corresponding lower flammability limits. It would then be possible to utilize the energy release from such exothermic reactions in conventional thermal power devices and heating furnaces. The practical limitations arise from the fact that gas-phase reactions, especially those of the common low molecular weight gaseous-fuels, such as methane in air proceed far too slowly to be a worthwhile practical source of energy release. Only through the use of sufficiently high reaction temperatures and avoiding having mixtures that are too lean that gas-phase reactions involving these fuels can proceed at rates suitable for practical exploitation (Wierzb *et al.*, 2003).

An effective pathway to utilize methane is its transformation into the synthesis gases (a mixture of CO and H_2), from which, further, hydrocarbons and methanol can be prepared. Currently, steam reforming is the dominant commercial process employed to produce the synthesis gas as seen in Equation 2.1 and 2.2.

$$CH_4 + H_2O \rightarrow CO + 3H_2 \qquad \Delta H^0_{298} = 206 \text{ kJ/mol} \tag{2.1}$$

However, this process is extremely endothermic and provides a syngas with a too high H_2/CO ratio for the Fischer-Tropsch and methanol syntheses. Recently, the partial oxidation of methane has attracted attention due to its mild exothermicity and suitable H_2/CO ratio (Wang *et al.*, 1999).

$$CH_4 + (1/2)\, O_2 \rightarrow CO+2H_2 \qquad \Delta H^0_{298} = -36 \text{ kJ/mol} \tag{2.2}$$

The overall production of methanol from natural gas, represented by methane, involves two steps: the endothermic reforming of natural gas and the exothermic synthesis reaction.

$$CH_4 + H_2O \rightarrow CO+3H_2 \qquad \Delta H^0_{298} = +206 \text{ kJ/mol} \tag{2.3}$$

$$CH_4 + 2H_2O \rightarrow CO_2+4H_2 \qquad \Delta H^0_{298} = +165 \text{ kJ/mol} \tag{2.4}$$

$$CO+2H_2 \rightarrow CH_3OH \qquad \Delta H^0_{298} = -90.6 \text{ kJ/mol} \tag{2.5}$$

The desired heat to drive the endothermic reforming reactions is provided by catalytic combustion in either a microchannel system or a cascade reactor sequence (Avcı, *et al.*, 2010):

$$CH_4 + 2O_2 \rightarrow CO_2 + 2H_2O \qquad \Delta H^0_{298} = -802.3 \text{ kJ/mol} \tag{2.6}$$

2.2. Catalysts

The catalysts for methane combustion can be divided into two groups: noble metals such as Pt, Pd, Rh, and Ru, and transition metal oxides such as Co_3O_4, CuO, Cr_2O_3 and MnO_2. Among the noble metal-based catalysts Pd-based catalysts always show the best activity in methane combustion. Transition metal oxides, however, show catalytic activity at relatively high temperatures (>700°C), and thus are not suitable for use in stainless steel microreactors due to low operating temperature limits (Guan *et al.*, 2008).

Among the transition metal oxide catalysts, cobalt-based oxides are ones of the most active catalysts in catalytic methane combustion, and Co_3O_4 is only slightly weaker than the noble metal catalysts for low temperature catalytic combustion (Jiang *et al.*, 2010). Precious metal catalysts possess a greater resilience against sintering and a higher resistance to sulfur poisoning, but more importantly a higher specific catalytic activity that renders them attractive as potential catalysts for catalytic combustion. They can be manufactured in a highly dispersed state on standard supports like silica and alumina, thus leading to improved activity (O'Connell *et al.*, 2009). Even though precious metal catalysts are better than transition metal oxides, it has recently been reported that palladium-supported catalysts have poor stability for methane conversion when the temperature is kept constant. Different additives, however, may be used to improve the palladium catalyst. One of the promising additives is Pt, which considerably improves the stability during reaction by preventing the aging of Pd catalysts (Persson *et al.*, 2007). Comparison between Pt/Al_2O_3 and Pd/Al_2O_3 catalysts shows that Pd is the most appropriate choice for lean reaction conditions and at low conversions under stoichiometric or rich conditions, whereas Pt/Al_2O_3 is more efficient at higher conversions with stoichiometric or rich conditions (Carlsson *et al.*, 2007).

Under fuel-lean conditions, Pd catalyst was the most active, although deactivation occurred above 650 ^{o}C, with reactivation upon cooling. Rh catalyst also deactivated above 750 ^{o}C, but did not reactivate. Pt catalyst was active above 600 ^{o}C. Fuel-lean reaction products were CO_2 and H_2O for all three catalysts. The same catalysts tested under fuel-rich conditions demonstrated much higher activity. In addition, a 'lightoff' temperature was found (between 450 and 600 ^{o}C), where a stepwise increase in reaction rate was observed. Following 'lightoff' partial oxidation products (CO, H_2) appeared in the mixture and their concentration increased with increasing temperature. All three catalysts exhibited this behavior (Lyubovsky *et al.*, 2003).

The most active catalysts for oxidation of saturated hydrocarbons, including CH_4, are the noble metals platinum and palladium where the latter in most cases is considered superior. The light-off temperature (T_{50} - the inlet gas temperature at which 50% conversion is achieved) for oxidation of methane over typical Pt/Al_2O_3 catalysts, is in the range of 625–725 K (Carlsson *et al.*, 2007).

The activity of Pt is mainly influenced by its oxidation state, with higher activities seen when Pt is less oxidized. Effectively, the electron deficiency of platinum varies with the electronegativity of additives, and the higher electronegativity enhances the electron deficiency of platinum, but depresses the oxidation of Pt (O'Connell *et al.*, 2009). Molybdenum helps to stabilize both the Pt and Al_2O_3 by enhancing the oxygen storage capacity and spillover effect, while on the other hand platinum maintains the surrounding molybdenum particles in its more active form (Da Silva *et al.*, 2003). It has also been suggested from density functional theory studies that MoO_3 supported Pt catalysts can facilitate single C–H bond activation in methane (Jiang *et al.*, 2007).

For methane oxidation under fuel-lean conditions, Pd-based catalysts are currently the only practical choice, because they can offer acceptable activity, lightoff temperature, and resistance to volatilization. Unfortunately Pd–PdO catalyst morphology and its reactions with methane is complex, and lead to complex behaviors such as deactivation at high temperature (above about 750 ^{o}C) and hysteresis in reaction rate through heating and cooling cycles. In

addition, lightoff and extinction temperatures are well above 300 ^{o}C for fuel-lean reaction on Pd-based catalysts, thus requiring the use of a preburner in many engine applications (Lyubovsky *et al.*, 2003).

A major challenge, then, is to limit the extent of reaction within the catalyst bed such that excessive heat does not damage the catalyst or substrate, yet release sufficient heat that downstream gas-phase combustion is stabilized at low flame temperatures for ultra-low emissions. To use a fuel-rich catalyst bed in a catalytic combustion system, additional air is introduced downstream of the catalyst so that combustion completion can occur fuel-lean. Based on this concept, fuel-rich catalytic reactors were tested by NASA and contractors for liquid fuel applications, and showed good soot-free performance (Brabbs *et al.*, 1993) (Rollbuhler *et al.*, 1991).

Fuel-rich operation provides greater catalyst activity, lower catalyst light off and extinction temperatures, and wider choice of catalyst type. For Pt, Pd and Rh catalysts greater activity to methane oxidation was found under fuel-rich conditions than under fuel-lean conditions. (Lyubovsky *et al.*, 2003), attribute this to different intermediate species adsorbed on the catalyst surface. Following the light-off, the surface is covered by oxygen when reacting with fuel-lean mixtures, while covered by CO and H species when reacting with fuel-rich mixtures.

Greater activity under fuel-rich conditions provides reduced catalyst lightoff and extinction temperatures for catalytic combustion systems. Absence of adsorbed surface oxygen minimizes catalyst loss through volatilization as precious metal oxide. Under fuel-rich conditions Rh catalyst showed the highest activity and the highest selectivity to partial oxidation products at temperatures above about 450 °C (after Rh 'lightoff'). Rh catalyst was more selective to partial oxidation products than Pt catalyst in partial oxidation of methane under short contact time conditions. Under fuel-rich conditions, two parallel reactions take place (Hickman *et al.*, 1993):

$$CH_4 + O_2 \rightarrow CO_2 + 2H_2O \qquad \Delta H^0_{298} = -802.3 \text{ kJ/mol} \tag{2.6}$$

$$CH_4 + 1/2O_2 \rightarrow CO+2H_2 \qquad \Delta H^0_{298} = -36 \text{ kJ/mol} \tag{2.7}$$

However, Pt has the lowest activity of the three tested catalysts at low temperature (less than about 700 °C). Between 450 and 600 °C, though, each catalyst exhibited a 'lightoff', where a stepwise increase in reaction rate is observed. Note that this 'lightoff' is not a thermal event (is not an effect of heat release on the catalyst surface) since the catalyst is in good thermal contact with the temperature-controlled electrically heated metal block. Thus, the observed stepwise increase in reaction rate occurred with incremental increase in catalyst temperature (Lyubovsky *et al.*, 2003). Similar behavior was reported (Burch *et al.*, 1994) for Pt catalyst under fuel-rich conditions, where they observed this type of 'lightoff' event at about 450 °C.

When compared to platinum, rhodium shows a higher methane conversion at a comparable temperature and also a higher selectivity to both CO and H_2. All differences are caused by the activation energy for methane decomposition which is higher on platinum than on rhodium. An additional explanation for the observed difference in the H_2 selectivity could be the higher activation energy for OH formation on rhodium compared to platinum. Conversion of methane as a function of temperature for rhodium (0.4 wt% Rh_2O_3) and platinum sponge (0.9 wt% PtO_2) was examined. Continuous flow experiment of CH_4/O_2 was at a feed molar ratio of 2. The oxygen conversion was complete in all experiments. Results showed that the conversion of methane is always higher for rhodium compared to platinum in the temperature range of 800 K up to 1000 K. The selectivities of H_2 and CO are also higher for rhodium compared to platinum. At 773 K the difference in H_2 selectivity amounts to 22%, while that to CO amounts to 16%. At 923 K, the difference in methane conversion between rhodium and platinum amounts to 15% and in the CO and H_2 selectivity was 25 and 7%. At a temperature of 1000 K the selectivity to CO and H_2 are comparable (Mallens *et al.*, 1997).

It was found that prior to catalyst 'lightoff' only CO_2 and H_2O were detected in the fuel-rich reaction product stream. Immediately after the 'lightoff' trace amounts of CO and H_2 were also detected, although CO_2 and H_2O remained the predominant reaction products. As the reactor temperature was further increased the concentration of CO_2 in the product stream

remained the same or even decreased, while the concentration of CO rapidly increased, indicating an overall increase in the reaction rate and process selectivity to partial oxidation products. Note that while CO concentration was increasing at higher temperatures after the 'lightoff', H_2 concentration remained at a trace level (Lyubovsky *et al.*, 2003).

A higher methane conversion than those obtained with stoichiometric and lean feed mixtures is observed under rich conditions, during an experiment carried out by performing lean pulses ($\lambda = 1.02$) in a constant rich feed gas ($\lambda = 0.98$). The analysis of reactants conversion and products distribution suggests that different chemistries are involved under lean and rich conditions. Only reactions of complete oxidation of H_2, CO, CH_4 and NO occur under excess of oxygen, whereas under rich conditions NO reduction, CH4 steam reforming and water gas shift also occur. In order to obtain further evidences on the relevance of SR and WGS reactions over the Pd/Rh-based catalyst, a sequence of tests was performed at different temperatures under stationary rich conditions ($\lambda = 0.967$) in absence of both O_2 and NO. Steady state values of CH_4, H_2 and CO outlet molar fractions are reported with respect to the monolith temperature. A decrease in CO molar fraction was detected starting from 335 ^{o}C, accompanied by an equimolar increase in H_2 outlet concentration. A minimum for CO concentration (0.116%) is reached at 435 ^{o}C, approaching thermodynamic equilibrium of WGS. It is worth noticing that at 435 ^{o}C also methane concentration starts to decrease due to the onset of steam reforming. At higher temperatures CO and H_2 outlet molar fractions increase while CH_4 is rapidly consumed indicating that the steam reforming effectively occurs, being likely promoted by Ce–Zr oxide and Rh, which are included in catalyst formulation (Bounechada *et al.*, 2012).

A novel catalytic combustion concept for zero emissions power generation has been investigated by Eriksson and his co-workers (2006). Catalysts consisting of Rh supported on ZrO_2, Ce-ZrO_2 or α-Al_2O_3 were prepared and tested under fuel-rich conditions for catalytic partial oxidation (CPO) of methane. The catalyst support material was found to influence the light-off temperature significantly, which increased in the following order Rh/Ce-ZrO_2 < Rh/ZrO_2 < Rh/α-Al_2O_3. The Rh loading, however, only had a minor influence i.e. an increase from 0.5 to 2% decreased the light-off temperature by 28 K. The high activity of Rh/Ce-ZrO_2

is probably related to the high dispersion of Rh on Ce-ZrO_2 and the high oxygen mobility of this support compared to pure ZrO_2. The formation of hydrogen was also found to increase over the catalyst containing ceria in the support material (Eriksson *et al.*, 2006).

2.3. Micro-reactor

Microstructured systems, generally known as micro reaction systems, are devices composed of structured flow paths having dimensions from sub-micrometer to sub-millimeter range that are fabricated by using methods of micro technology and precision engineering (Ehrfeld *et al.*, 2000). Micro channel technology is a novel approach in chemical processing hardware offering many advantages such as increased efficiency and productivity. This technology is characterized by the use of structured flow paths, i.e. channels with hydraulic diameters in the sub-millimeter range; characteristic diameters of microchannel reactors are between 10 to several hundred micrometers resulting in surface areas of 10000 - 50000 m^2/m^3 while in a conventional reactor this ratio is around 100 m^2/m^3 and rarely exceeds 1000 m^2/m^3 (Renken *et al.*, 2005).

Main advantages of microstructured reactors can be summarized as; size reduction through micro fabrication, reduced transport distances, enhanced heat and mass transfer rates and processing yields, reduced reaction volumes, controlled systems avoiding contamination and reducing safety risks, replacing a batch process by a continuous one and reduced chemical consumption (Charpentier *et al.*, 2007). These advantages are making use of microreactors possible in diverse applications such as highly exothermic reactions, screening for potential catalysts, precision particle manufacture, high throughput materials synthesis, fuel cell construction, miniature and portable micro plants (Wirth *et al.*, 2008).

The net result is volume reductions up to 90%, which leads to notable improvements in energy efficiency compared to the conventional process units (Lerou *et al.*, 2010). To illustrate, the size of a conventional steam reformer which has block dimensions around 30 m x 30 m x 30 m can be reduced to 3.9 m x 5.8 m x 3.9 m via the use of microchannels

(Tonkovich *et al.,* 2004).Significant compaction also offers the possibility of transporting the processing units (Seris *et al.*, 2008).

In a microchannel combustion system used as a heat source for other microdevices, catalytic combustion at relatively high concentration is needed. In this particular case, a reactor could minimize the possibility of explosion, due to its small reactor volume (Guan *et al.*, 2008).

Compact nature of the microchannel units favors heat transfer, which is important for highly exothermic and endothermic reactions in terms of effective catalyst utilization, favoring isothermal operation and preventing hot spots formation (Renken *et al.*, 2005, Hessel *et al.*, 2004). Making use of improved heat transfer properties, conversion of reactions when close to their thermodynamic equilibrium can be enhanced using channels for the heat exchange. Also this property gives the possibility to couple exothermic and endothermic reactions in a single reactor with heat exchanger design (Hessel *et al.*, 2004).

Multifunctional reactors hosting catalytic combustion and steam reforming of fuel at the opposite sides of a heat-exchanger appear to be very promising for achieving maximum compactness. Micro-channel reactors can satisfy this requirement because of their enhanced heat and mass transfer characteristics, the flow uniformity, the high surface area to volume ratio, safe control in explosive regimes and easier scale-up possibilities (O'Connell *et al.*, 2009).

The production of methanol requires syngas containing hydrogen and carbon monoxide at controlled temperatures. The supply of syngas from a combination of steam reforming and catalytic combustion of methane was modelled for a parallel microchannel array and for a cascade reactor system in which reaction occurs in a series of beds, heat exchange in interconnecting microchannel heat exchangers being used to maintain the desired temperature. Although conversion was slightly higher in the microchannel systems, the advantages of better temperature control and easy replacement of deactivated catalyst favoured the cascade array. (Avcı *et al.*, 2010).

Mass transfer, just like heat transfer, is better in microreactors. Since laminar flow is fully developed in microchannels the Sherwood number, which is mass transfer coefficient multiplied by hydraulic diameter divided by the diffusion coefficient, reaches a constant value. This implies that as the hydraulic diameter gets smaller; the mass transfer coefficient gets larger, decreasing the mass transfer limitation (Fichtner *et al.*, 2001).

In addition to the facts that hot-spot formation is avoided and the temperature control is well-established, flow amounts through the micro-flow units are considerably smaller when compared to the traditional reactors. These features give the opportunity of safer operations including the reactions characterized by near-explosive conditions, such as partial oxidations (Veser *et al.*, 2000).

Another beneficial feature of the micro sized units is the narrow residence time distribution. This increases the selectivity for production of specific material as it also enables easier scaling up by only increasing the number of units keeping the required geometry the same (Gandia *et al.*, 2009). Currently a number of chemical processes are operating batch-wise since desired capacity is not sufficient for a continuous process. Some of these processes have reaction times longer than their kinetic requirements because of slow mass and heat transfer and low specific surface area. Replacing these processes by a continuous one in a microreactor can decrease contact times significantly due to fast transport in thin fluid layers (Ehrfeld *et al.*, 2000).

Microchanneled reactors are significantly compact processing unit which offers the possibility of transportation (Seris *et al.*, 2008). Currently, chemical productions are carried out in large facilities, which are aimed to be as large as possible in terms of capacities due to economic reasons. However, as in case of petrochemical industries, raw materials need to be transported over long distances to a central plant, which makes a6vast number of small sized and remote feedstocks unprofitable. These feedstocks could be processed with microstructured systems since processing in microreactors requires less investments and operational costs (Ehrfeld *et al.*, 2000).

In a microchannel reactor, the catalyst support should be coated on the surface of the microchannel. To date, wash-coating and dip-coating have been the most common methods. Using these methods, a dense catalyst-coating layer could be successfully formed on the wall of a microchannel. The microreactor design was composed of two stainless steel plates with microchannels, which were jacketed in a stainless steel cell. Each plate had 14 microchannels of 25 mm long, with a semicircular cross-section (500 μm wide, 250 μm deep). Accordingly, the cross-sectional shape of the microchannel was circular.

Before preparation of the coatings in the microchannels, the plates were cleaned and thermally treated at 800 ^{o}C for 2 h, followed by clean treatment with distilled water and acetone. 0.5 g of γ-Al_2O_3 nanoparticles (Alfar Aesar, particle size = 8-14 nm) were dispersed into the mixture under stirring. After 24 h stirring at room temperature, the resulting suspension was introduced into the microchannels. It was found that the suspension could be moved along the microchannel automatically by capillary force from one side to the other. The coated plates were dried at 90 ^{o}C for 12 h and then heated to 300 ^{o}C in air and kept at this temperature for 2 h to burn out the PMMA particles. In order to remove all the organic components, the plates were further calcinated at 600 ^{o}C for 3 h.

Incipient wetness impregnation of Pd catalyst on the porous Al_2O_3 support layer in the microchannels was performed as follows: a calculated amount of aqueous solution of $Pd(NO_3)_2$ based on the weight of the Al_2O_3 layer was dropped into the layer, followed by drying at 120 ^{o}C for 12 h, and was then calcinated at 500 ^{o}C for 3 h. The Pd catalyst loaded on the Al_2O_3 layer in the microchannels was obtained in this manner. In this study, 1.0, 2.5, and 5.0 wt% Pd-loaded catalysts were prepared (Guan *et al.*, 2008).

At oxidation temperatures of 600 ^{o}C and above, rhodium interaction with the alumina support results in loss of reducibility and activity through inactive rhodium aluminate formation, and through increasing crystallinity of the alumina. Therefore, Rh/γ-Al_2O_3 is calcined at 500 ^{o}C. The calcination temperature range for Ru/Al_2O_3 catalysts is usually 450-570 ^{o}C for the same reasons. Pt/Al_2O_3 is also calcined at 500 ^{o}C following the practice in literature (Karakaya *et al.*, 2012).

3. EXPERIMENTAL WORK

3.1. Materials

3.1.1. Chemicals

Chemicals that are used for catalyst preparation are listed in Table 3.1.

Table 3.1. Chemicals used in catalyst preparation

Chemicals	**Formula**	**Grade**	**Supplier**	**Molecular Weight ($g.mol^{-1}$)**
Rhodium (III) nitrate solution	$Rh(NO_3)_3$	10%	Sigma-Aldrich	288.92
Ruthenium (III) nitrosyl nitrate	$Ru(NO)(NO_3)_x(OH)_y$ $x+y=3$	1.5%	Sigma-Aldrich	318.10
Tetraamine platinum (II) nitrate	$Pt(NH_3)_4(NO_3)_2$	99.99+%	Sigma-Aldrich	387.22
Aluminum Oxide	γ-Al_2O_3	99.98%	Alfa Aesar	101.96

3.1.2. Gases

Linde Gas Company (Istanbul, Turkey) is the supplier of the gases used in this study. Table 3.2 gives the specifications and the usage purposes of these gases.

Table 3.2. Specifications and applications of the gases.

Gas	Specifications	Application
Methane	99.700%	Reactant, GC calibration
Oxygen	99.990%	Reactant, GC calibration
Nitrogen	99.998%	Reactant (inert), GC calibration
Hydrogen	99.990%	Reducing agent, GC calibration
Carbon dioxide	99.990%	GC calibration
Helium	99.999%	GC carrier gas
Argon	99.999%	GC carrier gas

3.2. Experimental Set-Up

The experimental steps involved in this study can be described in five groups:

(i) Catalyst Preparation: This step involves incipient-to-wetness impregnation technique for preparation of catalysts.

(ii) Catalyst Coating and Microchannel Preparation: The aim of this step is to prepare the catalytic microchannel system that includes pretreatment of FeCrAl plates, blade coating of catalysts on plate and fitting plate into stainless steel cylindrical housing.

(iii) Catalyst Characterization: This step includes micro structural and elemental characterization of prepared catalyst.

(iv) Catalytic Reaction Step: The series of tests involved in this step is conducted in a continuous micro flow system which includes a stainless steel reactor fitted in a vertical furnace with temperature controlled heating connecting lines, mass flow controllers for inlet gases and a programmable temperature controller.

(v) Feed/Product Analysis: It includes analyzing reactant and product gas compositions with two online gas chromatographs that are connected in parallel and operated simultaneously.

3.2.1. Catalyst Preparation

The system that enables incipient-to-wetness impregnation method consists of:

(i) Vacuum flask, beaker (vacuum Erlenmeyer flask) and silicone tubing.

(ii) Retsch UR1 ultrasonic mixer, which provides uniform mixing and contact of metal precursor solution with support.

(iii) Vacuum pump, which removes air in the beaker to develop adhesion between support's porous structure and the precursor solution.

(iv) Masterflex computerized-drive peristaltic pump, which is used for the addition of the liquid solution of the metal precursor to the porous support material.

The catalyst preparation system is sketched in Figure 3.1. Detailed information about procedure is given in Section 3.3.

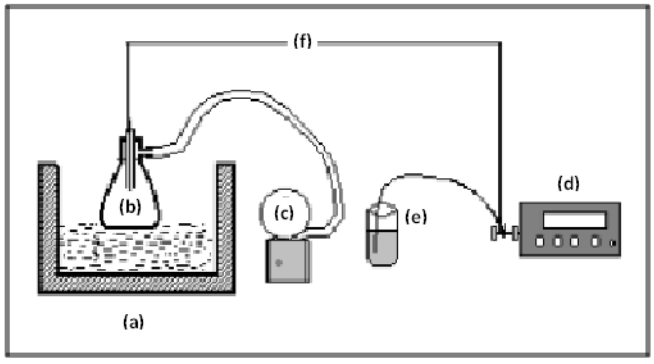

Figure 3.1. Impregnation system: (a) Ultrasonic mixer (b) Vacuum flask (c) Vacuum pump (d) Peristaltic pump (e) Beaker (f) Silicone tubing (Akın, 1996).

3.2.2. Catalyst Coating and Microchannel Preparation

FeCrAl sheets (Goodfellow Cambridge Limited) is cut into 2 mm x 5 mm x 20 mm plates by wire electro discharge machining method. Plate surfaces are cleaned with the sequential use of distillated water (for initial cleaning), HCl solution, distillated water (for removing HCl used in the previous step), ethanol and acetone. Surface cleaning avoids plates from undesired contaminants that can affect catalyst activity during the coating stage. After surface cleaning, plates are calcined at 900 ^{o}C for 2 hours to generate a native, corrugated Al_2O_3 structure that helps in ensuring better adhesion of the catalyst to the FeCrAl plate.

Catalyst powder that is prepared by impregnation method (see Section 3.3 for details) is turned into catalyst slurry by being mixed with deionized water at a water-to-powder weight ratio of 5–8:1. Blade coating on FeCrAl plates continued until weight per surface area 0.02 g_{cat}/cm^2. Coated plates dried to vaporize water and calcinated for removal of volatile components in slurry, and for thermal decomposition of precursor that exposes active metal part in catalyst. Detailed information was given in Section 3.3.2.

Coated single plate is inserted into 310-stainless steel cylindrical housing with 14.5 mm outer diameter and 30 mm length. Its inner structure, which is engineered by wire electro discharge machining, is suitable for both plate fitting and gas flow through micro-channel. Catalyst coating is made by forming 0.5 mm clearance from each edge on 5 mm width x 20 mm length plate for leading direct suit of catalyst layer into the micro-channel opening with the dimensions of 0.75 mm height, 4 mm width, and 30 mm length. Glass wool is stocked into the remaining 10 mm gap from the end of the plate to avoid any displacement that can be seen because of vertical positioning of plate in housing. All configurations about housing, plate and micro-channel are shown in Figure 3.2.

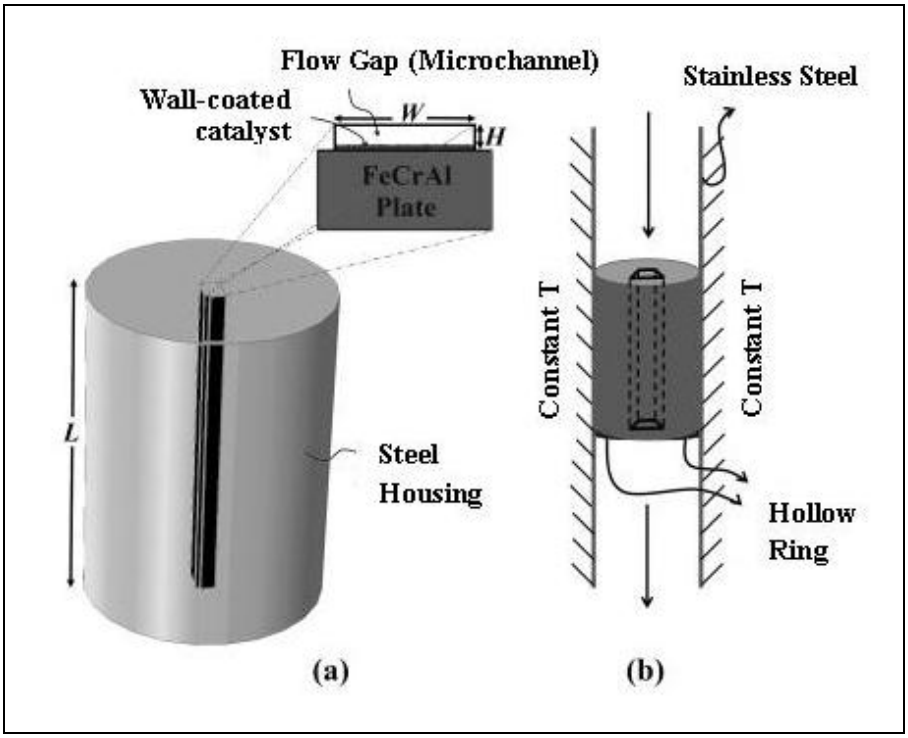

Figure 3.2. (a) Steel housing and the microchannel (b) Hollow tube (housing) inside the reactor.

3.2.3. Catalyst Characterization System

Catalyst characterization was examined by scanning electron microscope (SEM) and energy dispersive X-ray spectroscopy (EDX) (Philips XL30 ESEM-FEG/EDAX) analyses. SEM procedure shows the surface morphology of catalyst particles and determines the composition. EDX procedure is used to define elemental characterization of catalysts through mapping which shows distribution of elements in catalyst structure.

3.2.4. Catalytic Reaction System

Catalytic reaction system, which was designed and constructed in "Catalyst Technology and Reaction Engineering Laboratory (CATREL)", used in catalytic methane oxidation experiments is shown in Figure 3.3. Although Figure 3.3 contains gas chromatographs that are

used for analysis to maintain the integrity of system, reaction system was investigated as feed section and reaction section.

3.2.4.1. Feed Section. Research grade gases (H_2, O_2, N_2, CH_4) present in pressurized cylinders are metered and fed to the reaction system by Brooks 5850E mass flow control modules which are electronically set and controlled by four-channel Brooks 0154 control panel. Although the inlet pressures to the controllers are 30 psi, flow rate ranges are different for each gas. Specifications of the mass flow controllers are presented in Table 3.3. Connections between the gas cylinders are mass flow controllers are established via Swagelok fittings and tubes with appropriate dimensions (OD = 1/4", 1/8" or 1/16"). The mass flow controllers are calibrated *in situ* and their calibration curves are presented in Appendix A.

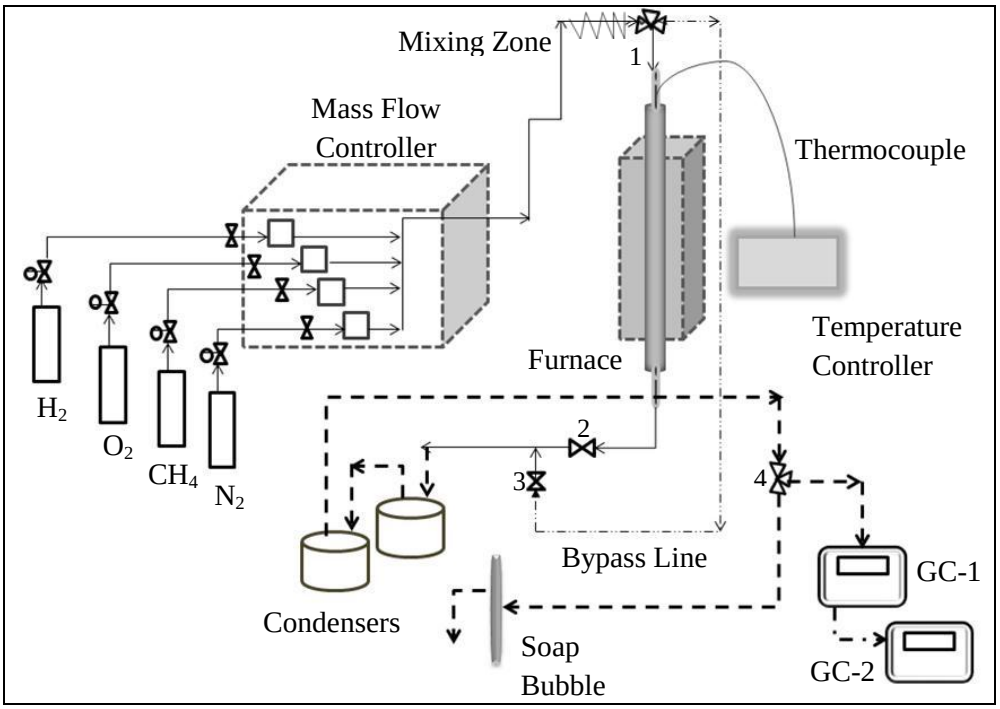

Figure 3.3. Catalytic reaction system.

At the inlet and the outlet of the mass flow controllers, 1/4" stainless steel tubing are used until the mixing zone, which is constructed using 1/16" stainless steel tubes after which

the diameter of connecting lines was gradually increased to 1/8" and 1/4". Before the reaction zone, gas flow can be diverted by a three-way valve (valve #1, Figure 3.3) either to the reaction section or to the bypass line which is used to analyze feed gas composition by gas chromatographs. An on-off valve (valve #3, Figure 3.3) is placed at the end of the bypass line. This valve prevents the product gases to fill the bypass line when it is not used (Şen, 2008).

3.2.4.2 Reaction Section. The reaction section consists of a 19.05 mm (1/2") OD stainless steel tube with 64 cm length and 1.65 mm wall thickness and a ceramic furnace (with 5 cm internal diameter and 50 cm length) in which the stainless steel tube is placed. The stainless steel housing including the catalytic plate and the microchannel (Section 3.4.2.2) is placed into the middle section of the stainless steel tube, which overlaps with the 10 cm long constant temperature zone of the furnace. In order to prevent the displacement of the housing during down flow position, diameter of the 34th cm (from the top) of the tube is narrowed down with a special method called metal spinning, such that this specific position became narrower than the diameter of the housing. The overlap between the machined part of the tube and the housing is sufficient to prevent any by-pass of the reactive flow from the gap between the housing and the tube.

Table 3.3. Specifications of the mass flow controllers.

Gas Type	**N_2**	**CH_4**	**O_2**	**H_2**
Flow Rate Range (ml min^{-1})	0-200	0-100	0-100	0-100
Upstream Pressure (psi)	30	30	30	30
Maximum Working Pressure (bar)	100	100	100	100
Ambient Temperature Limits (^{o}C)	5 to 65	5 to 65	5 to 65	5 to 65

As mentioned above, position of the reactor tube is adjusted to keep the catalytic microchannel at the constant temperature zone of furnace. Therefore, the reactor tube is positioned such that the top and bottom 7 cm parts are kept outside of the furnace. The tube is connected to the reaction system by using 1/4"-1/2" stainless steel Swagelok unions. Reaction

temperature was controlled to ± 0.5 K sensitivity by a Shimaden FP-21 programmable temperature controller and measured by a 1/16” K type stainless steel sheathed thermocouple which is positioned at the outer wall of the reactor tube section involving the catalytic microchannel. The gaps between the reactor tube and the furnace are insulated using ceramic wool to prevent heat loss and maintain stable temperature profile. At the end of the reactor an on-off valve (valve #2, Figure 3.3) is placed. It is kept closed during feed analysis to prevent back flow of the feed mixture coming from bypass line into the reactor (Şen, 2008).

3.2.5. Feed/Product Analysis System

The reactant and product gas streams are analyzed quantitatively using two different gas chromatographs, HP-Agilent 6850N and HP-Agilent 6890N. Both are temperature-controlled programmable network gas chromatographs, having thermal conductivity detectors (TCD). Methane and carbon dioxide are effectively analyzed using HP-Agilent 6850N that has a Porapak Q column with He carrier gas, whereas quantitative analysis of hydrogen and oxygen and other fixed gas are carried out by HP-Agilent 6890N that has a Molecular Sieve 5A column with Ar carrier. Molecular Sieve 5A column can be easily deactivated in the case of contacting with water vapor which is a product of methane oxidation. Therefore reactor exit line is connected to two salt-ice traps to remove water vapor in the product stream. An ice trap includes an insulated box filled with ice and a coiled tubing to increase the contact time between the gas flow and cold environment. Gas stream, which is either the product flow from the reactor or feed gas flow coming from the bypass line, is sent into a three way valve (valve #4, Section 3.3). This valve directs the flow to either the soap bubble flow meter for measuring the flow rate or to the gas chromatograph for gas analysis. Specifications and operating conditions of both gas chromatographs are listed in Table 3.4.

Table 3.4. Reactant and product gas analysis conditions.

GC Parameter	HP Agilent 6890 N	HP Agilent 6850 N
Detector Type	Thermal Conductivity	Thermal Conductivity
Column Oven Temperature	40^{o}C	40^{o}C
Injector Temperature	40^{o}C	110^{o}C
TCD Temperature	150 ^{o}C	150^{o}C
Carrier Gas	Argon	Helium
Carrier Gas Flow Rate	40 ml min^{-1}	20 ml min^{-1}
Column Packing Material	Molecular Sieve 5A, 60-80 mesh	Porapak Q, 80-100 mesh
Column Tubing Material	Stainless Steel	Stainless Steel
Column ID & Length	1/8" OD x 2 m	1/8" OD x 3 m
Sample Loop	1 ml	1 ml

Feed/product gases that are sent to gas chromatographs first enter to HP Agilent 6850 N and are then diverted to HP Agilent 6890 N by parallel connected line configurations which are shown in Figures 3.4 and 3.5.

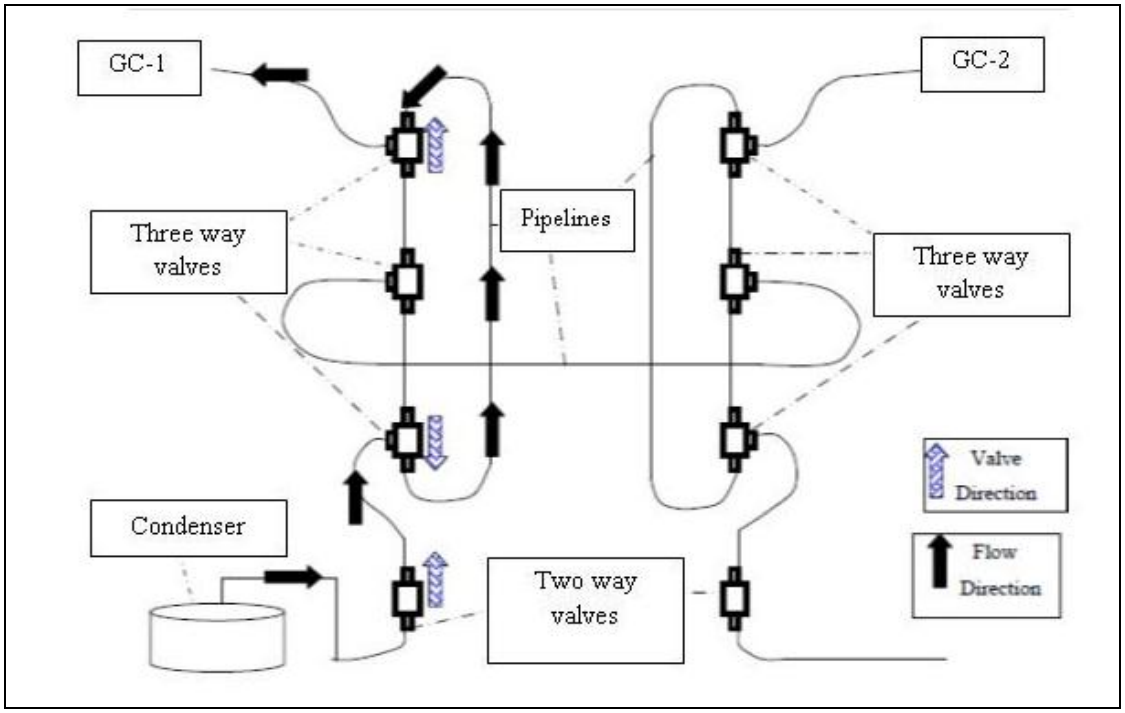

Figure 3.4. Flow routing arrangement for data analysis in HP Agilent 6850 N.

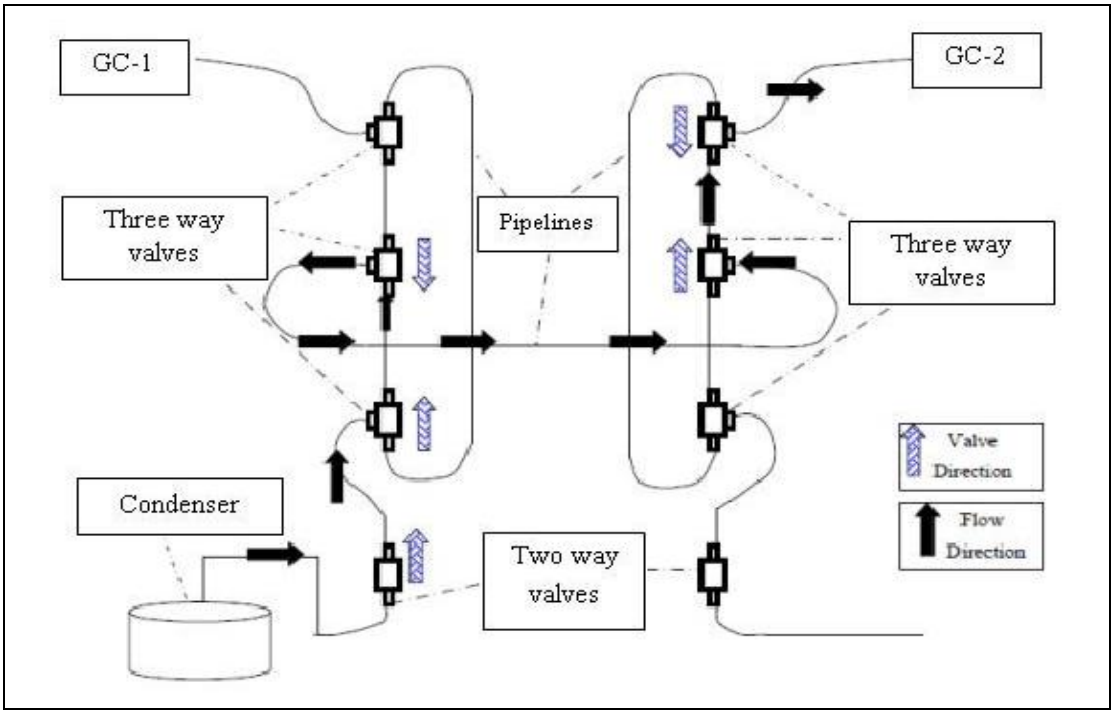

Figure 3.5. Flow routing arrangement for data analysis in HP Agilent 6890 N.

3.3 Catalyst Preparation

3.3.1 Support Preparation

The catalytic oxidation of methane is a high temperature reaction. Thus the catalyst support should have high thermal stability without sacrificing significantly from the surface area. γ-Al_2O_3 is a commonly used support material due to its high surface area. However, it is reported to have low stability at temperatures higher than 873 K and tends to facilitate carbon formation in the presence of steam due to its high acidity (Ma, 1995). The most thermally stable version of alumina is obtained when γ-phase is transformed into α-phase at temperatures higher than 1400 K (Doesburg *et al.*, 1999). However, its low surface area (< ca. 5 m^2/g) is likely to end up with poor catalytic activities due to the low dispersion of active metals. Hence, using a support such as δ-alumina (an intermediate phase between γ and α) having relatively high thermal stability and an acceptable surface area seems to be optimum in terms of obtaining efficient catalytic performance (Ma, 1995). In this study, alumina powder of 3 μm size (Merck, 120–190 m^2/g, γ phase) is used as supports for the catalysts. Thermally stable δ-phase of alumina is obtained by drying the γ-Al_2O_3 at 200^oC for 2 h and then calcining it at 900^oC for 4 h (Avci *et al.*, 2004).

3.3.2 Preparation of Pt/ δ-Al_2O_3

For catalytic oxidation experiments, 2 wt% Pt/δ-Al_2O_3 catalysts is prepared according to the incipient-to-wetness impregnation method by using aqueous solution of $Pt(NH_3)_4(NO_3)_2$. The support, δ-Al_2O_3 that is placed in a Büchner flask, is mixed ultrasonically under vacuum for 30 minutes. Precursor solution, which is prepared by dissolving calculated metal precursor in definite amounts of deionized water, is fed into the vacuumed flask by Masterflex computerized-drive peristaltic pump at a rate of 0.5 mL/min via silicone tubing.

Vacuum pump is used to remove the trapped air in the pores of the support that could prevent penetration of the solutions. Furthermore vacuum pump gives a uniform distribution

of the active component. Hence it is used not only before addition of precursor solution but also during and after the impregnation step. The resulting thick slurry, which is formed after ultrasonic mixing of the aqueous solution and the support under vacuum for 1.5 h, is then dried overnight at 393 K and calcined at 773 K for 4 h to obtain Pt/δ-Al_2O_3 particulate form.

The next step involves the preparation of the aqueous coating slurries that is explained in Section 3.2.2. The first step in the preparation of the slurry involves mixing of 3 μm catalyst powders with deionized water at a water-to-powder weight ratio of 5–8:1. The slurries are then blade-coated repeatedly onto the 5 mm × 20 mm plates until the weight per surface area reaches ca. 0.02 gcat/cm^2. The coated plates are dried overnight at 120^oC, and calcined for 4 h at 500^oC. After this step, coated plates become ready for being inserted into the metallic housing mentioned in Section 3.2.2. The same procedure is employed also for coating Rh/δ-Al_2O_3 and Ru/ δ-Al_2O_3 catalysts, with each of them containing 2 wt% of active metal. Detailed information about quantities is shown in Table 3.5.

Table 3.5. Prepared catalysts.

		Catalyst	
	Pt/ δ-Al_2O_3	**Rh/ δ-Al_2O_3**	**Ru/ δ-Al_2O_3**
Composition	Support: %98 Metal: %2	Support: %98 Metal: %2	Support: %98 Metal: %2
Precursor	$Pt(NH_3)_4(NO_3)_2$	$Rh(NO_3)_3$	$Ru(NO)(NO_3)_x(OH)_y$ x+y=3
Precursor Form	Solid	Liquid	Liquid
Prepared Catalyst Amount	2 g	2 g	2 g
Precursor Amount	0.079 g	0.284 ml	2.492 ml
Amount of deionized water for precursor solution	1.1 ml/g support	1.2 ml/g support	none

3.3.3 Pretreatment

After the calcination of coated plates, catalysts are usually inactive because of being in their oxide forms. In order to obtain high catalytic activities, a pretreatment involving the reduction of the active metals, from the oxide state to the metallic state, is required prior to the reaction. (Ma *et al.*, 1995) reported that during reduction the water in the catalysts may cause premature sintering, which may lead to deactivation before the reaction. Considering these issue, the following stepwise reduction procedure is followed for the catalyst used in all of the experiments.

After placing the housing that contains catalyst coated plate into the constant temperature zone of the microreactor, N_2 is allowed to flow at 20 ml/min for 10 minutes to remove oxygen from the system. The temperature was increased from room temperature to 773 K followed by 15 minutes isothermal segment. Then the gas flow is switched from N_2 to H_2 and the H_2 flow rate is set to 40 ml/min. Reduction continues at the constant temperature of 773 K for 2 hours. After reduction, the system is allowed to cool down to 523 K under N_2 flow at 20 ml/min. Below this temperature, the gas flow was decreased from 20 ml/min to 5 ml/min, the latter which is allowed to flow overnight to sweep H_2 from the system prior to the tests.

3.4 Reaction Tests

3.4.1. Preliminary Work

Before starting the experiments, gas chromatographs are calibrated by injecting known amounts of the species separately to the chromatographic column under the conditions given in Table 3.4 and by reading the corresponding retention time and the area under the peak calculated by computer software. Using this procedure, peak area versus volume % graphs were constructed for each gas and the corresponding calibration curves were determined by linear regression. Appendix B. gives chromatographs calibration curves for each gases using peak area versus volume % graphs to calculate gas mole numbers.

3.4.2. Blank Tests

Blank tests are conducted to ensure that the material of construction, ceramic wool, FeCrAl plates and housing material did not interfere with the reaction test outputs. The results indicate that these items above are inactive under the conditions used in the reaction experiments.

3.4.3. Catalytic Oxidation of Methane

Methane conversion is investigated under fuel rich feed stream conditions. In all experiments amount of catalyst ($Pt/\delta\text{-}Al_2O_3$, $Rh/\delta\text{-}Al_2O_3$, $Ru/\delta\text{-}Al_2O_3$) that is coated on a FeCrAl plate stayed in the range of 29 mg to 35 mg. As explained in Section 3.4.2, the catalyst is pretreated through reduction by 40 ml/min H_2 flow for 2 hours. In order to determine catalyst effect on methane conversion at oxidation reactions, two different experimental plans are employed. In the first plan, four different inlet molar CH_4/O_2 ratios, 1.32, 1.59, 1.85 and 2.13, are applied at a constant total feed flow 100 ml/min by increasing reaction temperature from 623 K to 923 K for all three catalysts. The other plan consisted of keeping CH_4/O_2 ratio at a constant value as 1.85 while changing feed flow stream to 75, 100 and 125 ml/min through increasing reaction temperature from 623 K to 923 K.

For every catalyst-feed mixture combination, temperature program is applied, and product samples are analyzed at definite time intervals of 20-25 min. By the time desired amount of homogeneous mixed feed gases directed to reactor by valve 1 (Figure 3.3), the reaction temperature is firstly increased from room temperature to 623 K at a rate of 3 K/min followed by 10 min isothermal segment. From 623 K to 923 K, the reaction temperature was increased at a rate of 1 K/min to enable definite time intervals 20-25 min for sending product gases to GC analysis through changing valve 4 from ventilation to gas chromatographs. At the end of product analysis, valve 1 is diverted to bypass line, valve 3 is opened to allow the exit of feed gases and valve 2 is closed to prevent back flow of feed gases to the reactor. Finally, the feed gas analysis is completed by changing the position of valve 4 from ventilation to gas

chromatographs and the reactor is set to cool down while N_2 gas is diverted into the reactor to sweep product gases.

Product gases are collected between 623 K and 923 K to obtain conversion values at different temperatures by diverting exit product stream to gas chromatographs by valve 4. Parallel operation of the GCs is initiated by diverting the product stream initially to GC-1 using the three way valves (Figure 3.4). Before injection of the sample collected in the sample loop, product gases are allowed to flow into GC-1 (Porapak Q column) for 1 min. to enhance exact combination result of the product gases in the distinct temperature. After injection to GC-1, product gases are then diverted into GC-2 (see Figure 3.5) followed by charging into same loop and sample injection into Molecular Sieve 5A column. Analysis is finished by diverting the product flow to the ventilation through valve 4. This analysis procedure is repeated in every 20-25 min during the course of the reaction carried out between 623 K and 923 K. Details of the analysis conditions are given in Table 3.4. Methane conversion is defined and calculated as follows.

$$CH_4 conversion(\%) = \frac{[CH_4]_{in} - [CH_4]_{out}}{[CH_4]_{in}}$$

4. RESULTS AND DISCUSSION

4.1 Effect of Inlet CH_4/O_2 Ratio on Methane Conversion

The effects of inlet molar ratio of methane-to-oxygen on methane conversion are investigated over Pt, Rh and Ru-based coated catalysts in the microchannel reactor. The oxidation of methane can be described by the following reaction:

$$CH_4 + 2O_2 \rightarrow CO_2 + 2H_2O \qquad \Delta H^0_{298} = -802.3 \text{ kJ/mol} \tag{4.1}$$

Experiments are conducted under fuel rich conditions that involve methane-to-oxygen ratios greater than the stoichiometric value of 0.50. Oxygen is the limiting reactant hence methane conversion is dictated by the amount of oxygen existing in feed stream. Maximum conversion that can be achieved is equal to:

$$\frac{1}{2 \times [CH_4 : O_2]} \times 100$$

Therefore actual CH_4 conversion is normalized using maximum value to define the conversion in this study (Avcı *et al.*, 2003):

$$Conversion = \frac{Actual\ hydrocarbon\ conversion}{Maximum\ attainable\ hydrocarbon\ conversion} \times 100$$

Figure 4.1 shows methane conversions obtained over Pt/δ-Al_2O_3 catalyst at different CH_4/O_2 ratios with increasing temperature. Total feed flow kept constant at 100 ml/min. The ratio change is adjusted by changing the O_2 flow and balancing it with the N_2 flow to keep the total flow rate constant. In all experiments methane flow rate is kept constant at 21.8 ml/min. Methane conversion is found to increase with temperature regardless of the feed composition.

This finding is linked with the positive dependence of reaction rate with temperature. Between 650 K and 800 K, conversion is found to follow the decreasing CH_4/O_2 order of 2.13 > 1.59 > 1.85 > 1.32. However, this trend begins to change after 800 K (except for CH_4/O_2=1.85), and at 850 K conversion follows the decreasing CH_4/O_2 order of 1.32 > 1.59 > 2.13. The activity of Pt is mainly influenced by its oxidation state, with higher activities seen when Pt is less oxidized (O'Connell *et al.*, 2009). Although methane conversion at CH_4/O_2=1.85 is the highest between 800 K and 900 K, result could not stay stable for changing temperature among all results.

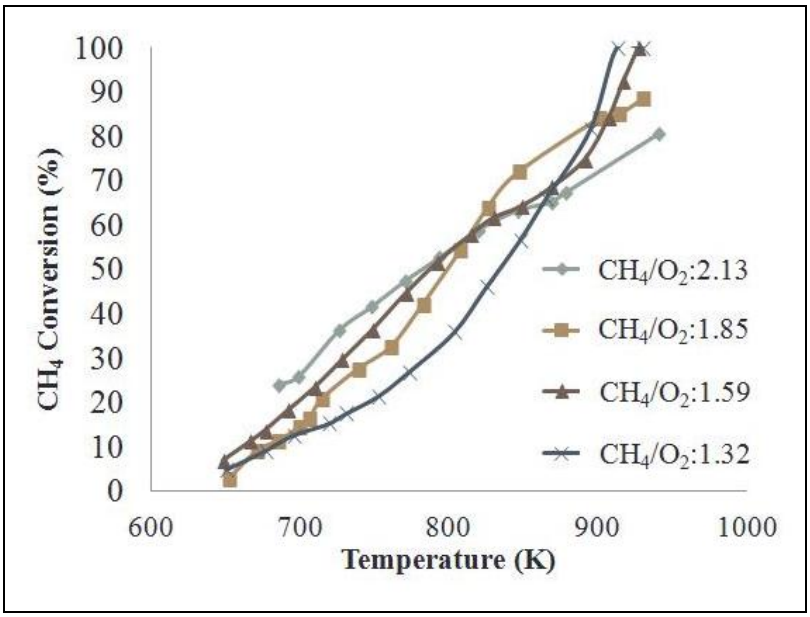

Figure 4.1. Methane conversion vs. temperature obtained over Pt/δ-Al_2O_3 at different CH_4/O_2 ratios (Total feed flow=100 ml/min).

Methane conversions obtained over Rh/δ-Al_2O_3 coated microchannel at different CH_4/O_2 ratios with increasing temperature are given in Figure 4.2. Below 750 K, temperature change gave almost the same methane conversions in all cases; conversion trend lines for different CH_4/O_2 ratios overlap with each other until 750 K. After this temperature, differences between the conversion curves became notable and methane conversions decreased in the CH_4/O_2 order of 2.13 > 1.85 > 1.59 > 1.32. For all ratio values (except for 1.32) conversion

reached 100%. It is reported that, under fuel-rich conditions, Rh catalyst showed the highest activity and the highest selectivity to partial oxidation products at temperatures above ca. 723 K (Hickman *et al.*, 1993). When compared to Pt and Ru catalyst, methane conversions obtained at 823 K over Rh are 80% and 100% for CH_4/O_2 equal to 1.85 and 2.13, respectively. However, conversion stays between 30-40% for Ru and 60-70% for Pt at same temperature and CH_4/O_2 values (Figures 4.1, 4.2 and 4.3).

When compared to Pt, Rh shows a higher methane conversion at a comparable temperature and also a higher selectivity to H_2 which is showed by Figure 4.8. in Section 4.2. The differences can be attributed to the activation energy for methane decomposition which is higher on platinum than on rhodium (Mallens *et al.*, 1997). In contrast with the other catalysts, at different CH_4/O_2 values, temperature increase led to the evolution of similar conversion curves over $Ru/\delta\text{-}Al_2O_3$ (Figure 4.3).

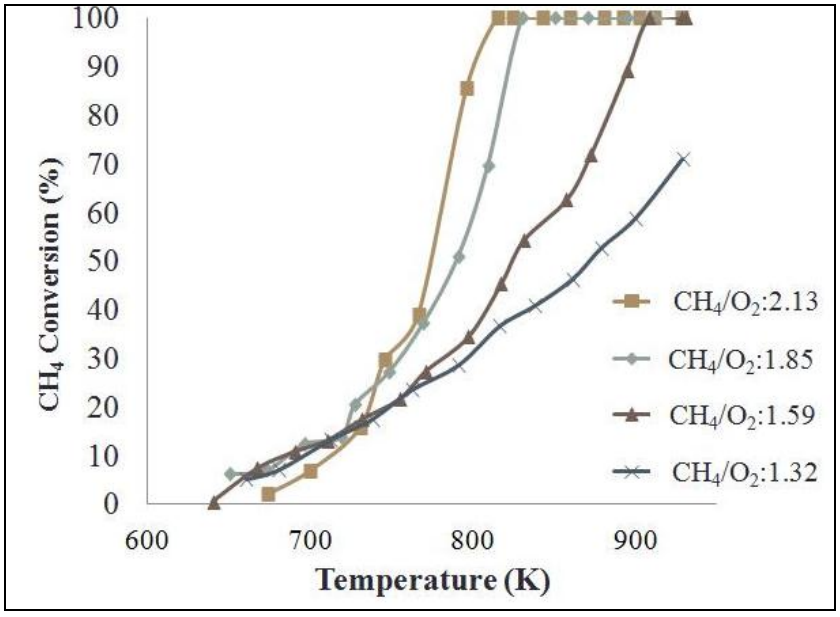

Figure 4.2. Methane conversion vs. temperature obtained over $Rh/\delta\text{-}Al_2O_3$ at different CH_4/O_2 ratios (Total feed flow=100 ml/min).

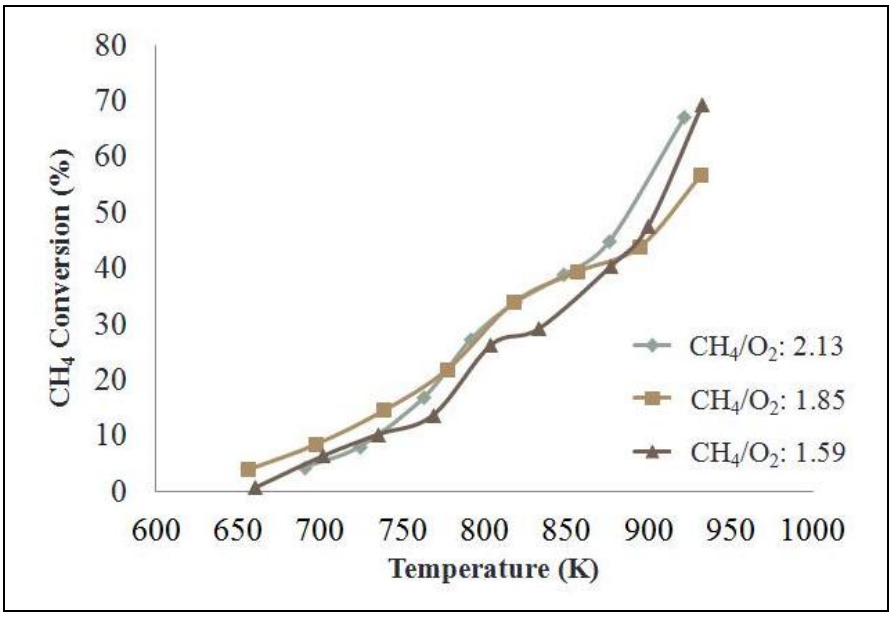

Figure 4.3. Methane conversion vs. temperature obtained over Ru/δ-Al_2O_3 at different CH_4/O_2 ratios (Total feed flow=100 ml/min).

The quantitative variations between light-off temperatures of different catalysts are represented in Table 4.1 and in Figure 4.4. In this study, the light-off temperature is defined at which 10% of methane conversion is achieved (T_{10}). The definition is based on that of Ma and co-workers (1996), but the definition based on 50% conversion is also used in the literature. For example, the light-off temperature (T_{50} - the inlet gas temperature at which 50% conversion is achieved) for oxidation of methane by oxygen over typical Pt/Al_2O_3 catalysts is reported to be in the range of 625–725 K (Carlsson *et al.*, 2007). In addition, a 'lightoff' temperature was found between 450 and 600^oC for Pd, Pt and Rh catalysts under fuel rich conditions. (Lyubovsky *et al.*, 2003). The outcomes of this study show that as the amount of oxygen used in feed stream is increased, light-off temperatures are generally found to decrease to a certain value then start to increase again for all three catalysts (Table 4.1, Figure 4.4). The formation of minimum light-off temperatures is observed to be at CH_4/O_2 ratios of 1.6 for Pt/δ-Al_2O_3 and Rh/δ-Al_2O_3, and 1.82 for Ru/γ-Al_2O_3.

Moreover, catalytic activity is found to follow the decreasing order of Pt/δ-Al_2O_3 > Rh/δ-Al_2O_3 > Ru/δ-Al_2O_3 with respect to light-off temperature. The trend observed in Figure 4.4 can be explained by the competitive adsorption between methane and oxygen molecules (Avci *et al.*, 2003). At high oxygen quantities in the feed (i.e. at low CH_4/O_2 ratios) catalyst surface tends to be occupied by oxygen and the number of sites for methane adsorption is scarce. The opposite of this trend occurs when the feed is rich with methane (i.e. at high CH_4/O_2 ratios). This phenomenon leads to the evolution of an optimum CH_4/O_2 ratio leading to the highest reaction rate, hence the lowest light-off temperature. Pt/Al_2O_3 is reported to be more efficient at higher conversions with stoichiometric or fuel rich conditions (Carlsson *et al.*, 2007).

Table 4.1. Temperatures specific to Pt-, Rh- and Ru-coated microchannel driven methane conversions of 10%, 20%, 30% and 50%.

Catalyst	**CH_4/O_2**	**T_{10} (^oC)**	**T_{20} (^oC)**	**T_{30} (^oC)**	**T_{50} (^oC)**	**Total feed flow (ml/min)**	**CH_4 feed flow (ml/min)**
2% Pt/Al_2O_3	1.86	402	440	477	523	100	21.8
	1.59	386	427	456	514	100	21.8
	1.32	407	472	510	560	100	21.8
2% Rh/Al_2O_3	2.13	441	464	474	503	100	21.8
	1.85	414	453	482	516	100	21.8
	1.59	408	470	506	551	100	21.8
	1.32	422	476	522	600	100	21.8
2% Ru/Al_2O_3	2.13	461	500	531	614	100	21.8
	1.85	436	496	531	640	100	21.8
	1.59	460	513	565	631	100	21.8

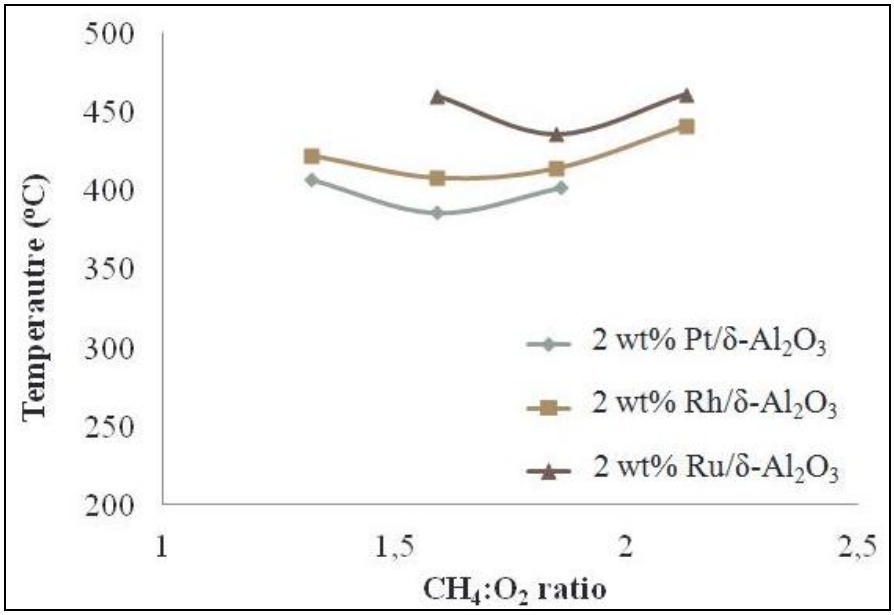

Figure 4.4. Light-off temperatures (T_{10}) versus CH_4/O_2 ratio obtained over Pt, Rh and Ru-coated microchannels.

4.2 Effect of Total Flow Rate on Methane Conversion

The effect of total flow rate on methane conversion obtained over Pt, Rh and Ru-based microchannels are presented in Figures 4.5, 4.6 and 4.7, respectively. In all experiments, CH_4/O_2 ratio is kept constant at 1.85 and total feed flow rate is varied as 75, 100 and 125 ml/min.

The response of Pt-coated microchannel against temperature increase at different total flow rates is given in Figure 4.5. It can be observed that methane conversion increases quickly when the total flow rate is 75 ml/min, whereas no important difference is noted between 100 and 125 ml/min. Faster increase in conversion at 75 ml/min can be explained by the residence time effect, which leads to higher conversions due to longer contact of reactive flow with the Pt-catalyst layer. As the contact is reduced at 100 ml/min, conversions turn out to be less responsive against temperature change. However, further increase of 25 ml/min in the total flow rate did not affect conversion-temperature trend.

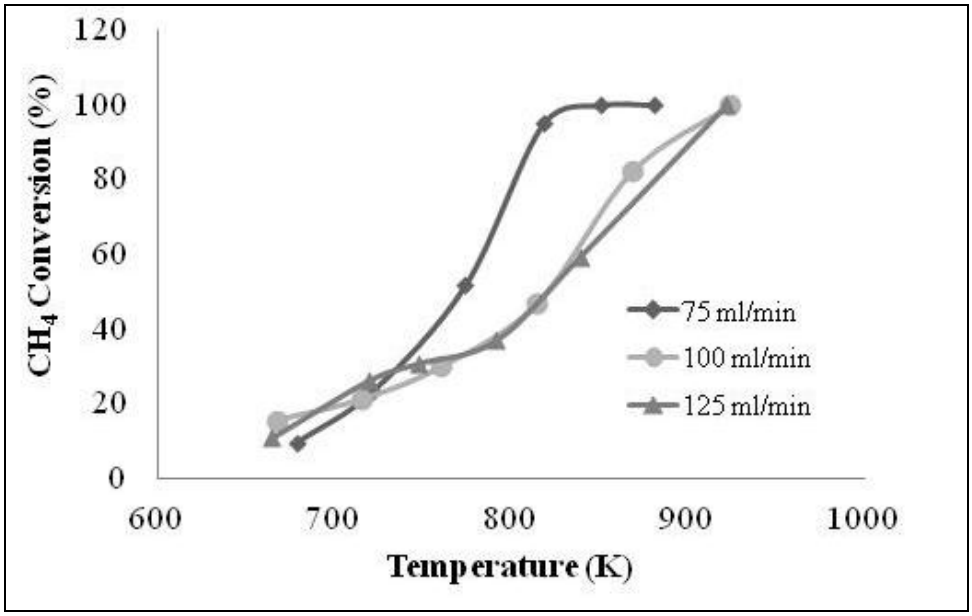

Figure 4.5. Methane conversion vs. temperature obtained over Pt/δ-Al_2O_3 at different total feed flow rates (CH_4/O_2 =1.85).

Figure 4.6 shows the methane conversion-temperature curves obtained over Rh-coated microchannel at different total flow rates. Although the positive dependence of conversion on temperature is common with those of other catalysts, the highest rate of increase in conversion is observed at 100 ml/min. In other words, in contrast with Pt (Figure 4.5), shifting the total flow rate from 75 to 100 ml/min have led to higher conversions at identical temperatures. The results can be explained with high activity characteristics of Rh, which is capable of converting increased amounts of reactive flow.

However, a further increase in total flow rate to 125 ml/min led to a decrease in conversion which is a result of reduced contact time that outperformed the catalytic activity of Rh. The third coated catalyst, Ru, is found to behave similar to the Pt-coated microchannel against changes in total flow rate (Figure 4.7). Reduction in the contact time turned out to be significant enough to outperform the catalytic activity of Ru.

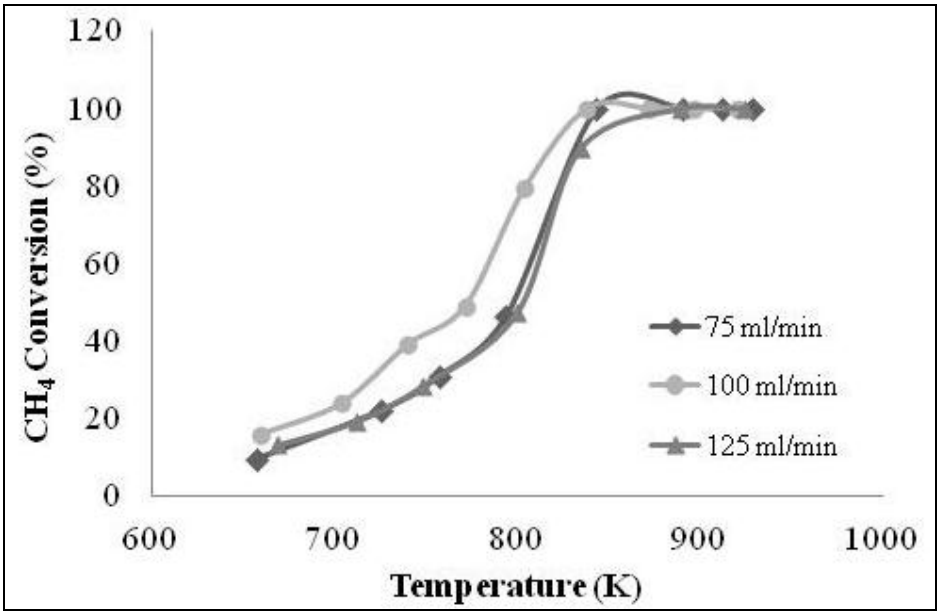

Figure 4.6. Methane conversion vs. temperature obtained over Rh/δ-Al_2O_3 at different total feed flow rates (CH_4/O_2 =1.85).

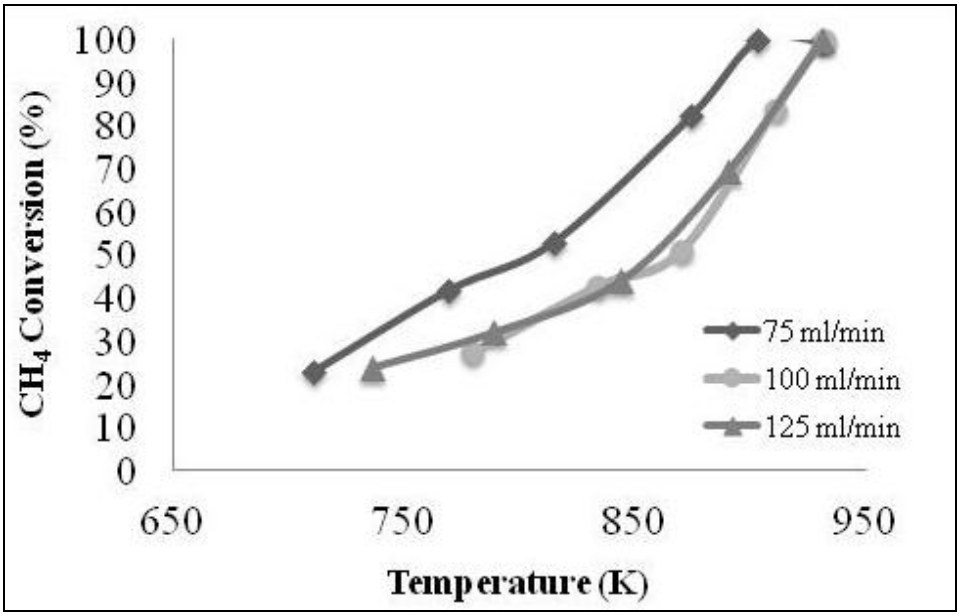

Figure 4.7. Methane conversion vs. temperature obtained over Ru/δ-Al_2O_3 at different total feed flow rates (CH_4/O_2 =1.85).

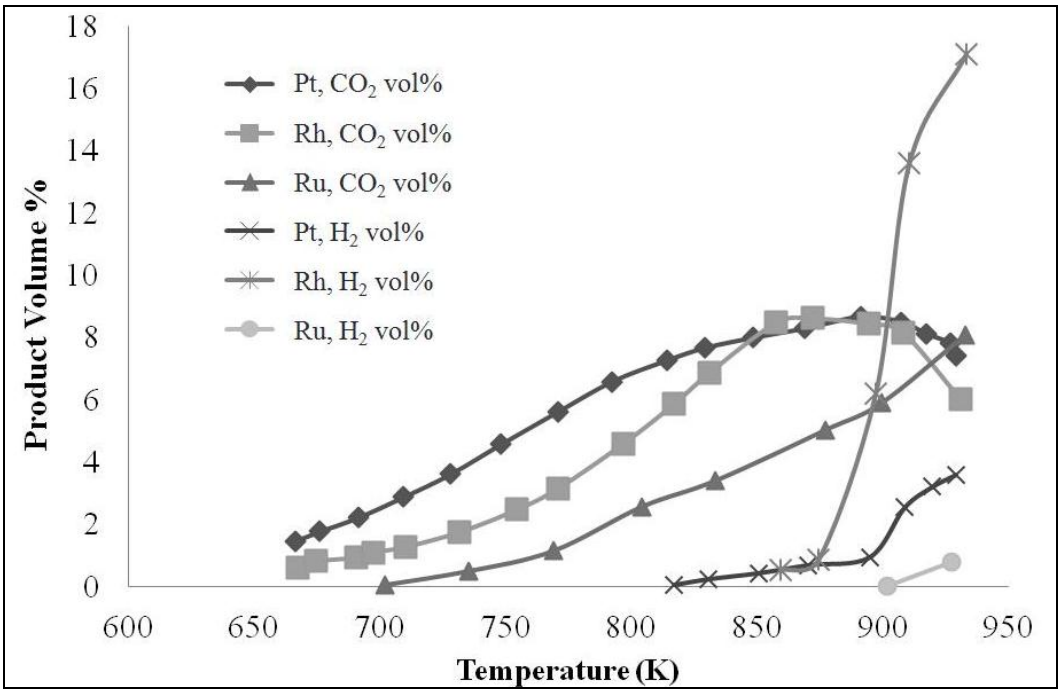

Figure 4.8. Vol.% of H_2 and CO_2 with respect to increasing temperature (CH_4/O_2 = 1.59, total feed flow rate = 100 ml/min).

Figure 4.8 explains that at high temperatures, oxidation reaction produced H_2 other than CO_2 and H_2O for all three catalysts. While the product CO_2 start to decrease for Pt and Rh catalysts between 800 and 850 K, H_2 production rate increases gradually. According to the results of Hickman and co-workers (1993), total oxidation and partial oxidation reactions take place together under fuel rich conditions. It is also reported that prior to catalyst 'light-off' only CO_2 and H_2O are detected in the fuel-rich reaction product stream, but, immediately after the 'light-off', trace amounts of CO and H_2 are also detected (Lyubovsky *et al.*, 2003). Bounechada and co-workers (2012) explain that under fuel rich conditions in the absence of both O_2 and NO and at higher temperatures, CO and H_2 outlet molar fractions increase while CH_4 is rapidly consumed indicating that the steam reforming effectively occurs. It is also worth noting that fraction of H_2 in the product stream obtained over Rh is significantly higher than those produced over Pt and Ru. This is linked with the fact that Rh favors direct conversion of methane to synthesis gas ($CH_4 + 0.5O_2 = CO + 2H_2$) at high temperatures and under fuel rich conditions, whereas Pt favors total oxidation stoichiometry (Reaction 4.1)

(Hickman *et al.*, 1993). These interpretations can also be supported by CO_2 fractions, which decreases much more rapidly over Rh at temperatures higher than 850 K (Figure 4.8).

4.3. Catalyst Characterization Tests

Characterization of the wall-coated catalysts are carried out by scanning electron microscopy (SEM) and energy-dispersive X-ray spectroscopy (EDX) (Philips XL30 ESEM-FEG/EDAX) analyses. Theoretically all catalysts used in the experiments are aimed to have 2% metal content by weight. For a proper evaluation on catalytic activity performance, metal content of each prepared set of catalyst is analyzed to measure the actual metal content. The analyses also give the chance to make a proper comparison between catalysts used in oxidation reactions and the catalyst that are only reduced but not used in reactions, which are called spent and fresh catalysts, respectively. The catalysts are compared on the basis of metal dispersion on the surface, metal content and the morphology of metal content.

Table 4.2 summarizes metal content differences between fresh and spent catalyst samples. Both fresh and spent catalysts nearly involve the target metal content of 2% by weight. When the spent catalysts are compared with each other, it can be noted that the deviation in metal contents of Ru catalysts is higher than those of Pt and Rh. In other words, the homogeneity of Ru dispersion is low when minimum and maximum values are compared. This observation may help in explaining the low catalytic performance of Ru-coated microchannel in the catalytic oxidation tests.

Another finding that can be extracted from Table 4.2 is related with the decrease of Pt and Rh metal content during the reaction. Comparison of the average metal contents of fresh and spent samples shows that, some oxidation might have taken place and has converted reduced metals to their oxide state. Even though Pt and Rh are noble metals, i.e. are known with their resistance against oxidation, some decrease in metal content should be expected as the catalysts are tested for a series of experiments without being removed from the reactor. This trend, however, is not clearly observed for Ru, possibly due to its different characteristics in methane oxidation.

Table 4.2. Metal contents of the fresh and spent prepared catalysts.

	Fresh Catalyst			Spent Catalyst		
	Minimum Metal %	**Average Metal %**	**Maximum Metal %**	**Minimum Metal %**	**Average Metal %**	**Maximum Metal %**
2% Pt/δ-Al_2O_3	1.85	2.36	2.65	1.35	1.91	2.33
2% Rh/δ-Al_2O_3	1.62	2.03	2.37	1.4	1.83	2.34
2% Ru/δ-Al_2O_3	1.63	1.76	1.85	1.04	2.21	3.07

For a better understanding of the degree of metal dispersion, SEM images and EDX mapping of the catalysts samples are provided in Figures 4.9-4.13. Bright spots on SEM images show the metal existence, whereas the small spots in EDX maps (Figures 4.9b-4.13b) indicate the degree of metal dispersion.

EDX mapping of fresh and spent Pt catalysts are given in Figures 4.9 and 4.10, respectively. Pt content of fresh catalyst and spent catalysts are determined as 2.58% and 2.27% (by weight) as a result of EDX analysis. Dispersion of Pt in both fresh and spent catalyst samples seems to be homogeneous. Moreover, particle size of Pt seems to remain almost unchanged after the reaction, which shows that the catalyst is not deactivated by sintering (i.e. coalescence) of the metal particles.

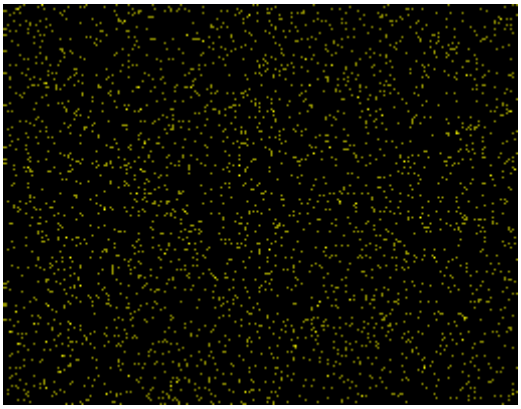

Figure 4.9. EDX mapping of Pt/δ-Al_2O_3 with 2.58 wt% Pt content (fresh catalyst).

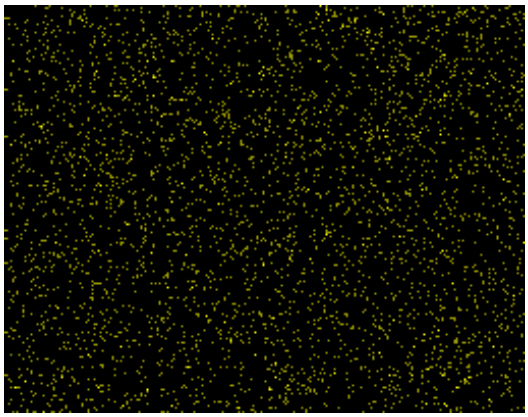

Figure 4.10. EDX mapping of Pt/ δ-Al_2O_3 with 2.27 wt% Pt content (spent catalyst).

Observations for the Pt catalyst outlined above are also valid for the fresh and spent Rh/δ-Al_2O_3 catalyst, whose EDX mappings are shown in Figures 4.11 and 4.12. EDX analyses show that the metal contents of the fresh and spent catalysts are 2.19 and 2.34%, respectively. In addition to the improved dispersion, mapping results of Rh demonstrate no metal agglomeration. This observation, which is also stated for Pt, can explain enhanced catalytic activity of Pt and Rh during methane oxidation.

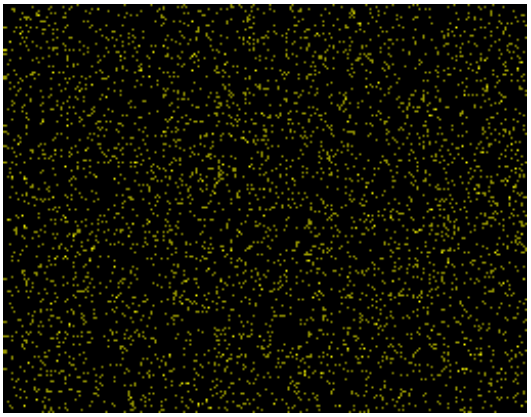

Figure 4.11. EDX mapping of Rh/δ-Al_2O_3 with 2.19 wt% Rh content (fresh catalyst).

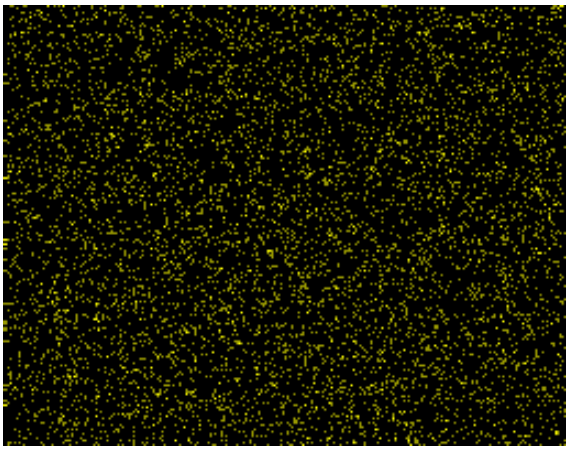

Figure 4.12. EDX mapping of Rh/δ-Al_2O_3 with 2.34 wt% Rh content (spent catalyst).

Figures 4.13 and 4.14 give the EDX mappings of the fresh and spent Ru/δ-Al_2O_3 samples. Ru metal content is found to be 1.85 and 1.04% in fresh and spent catalysts, respectively. When compared to Rh and Pt, Ru catalyst has a lower metal content, which should normally demonstrate better dispersion characteristics. However, mapping results of the Ru catalysts do not reflect good dispersion. It can be observed that Ru metal tends to agglomerate on the support layer of both fresh and spent samples. This can provide some explanation about the lower catalytic activity of Ru in methane oxidation.

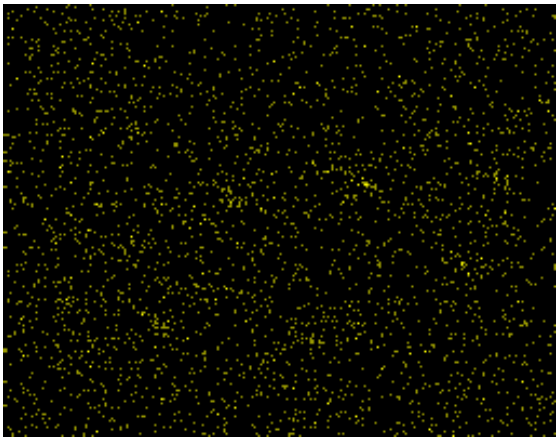

Figure 4.13. EDX mapping of Ru/ δ-Al_2O_3 with 1.85 wt% Ru content (fresh catalyst).

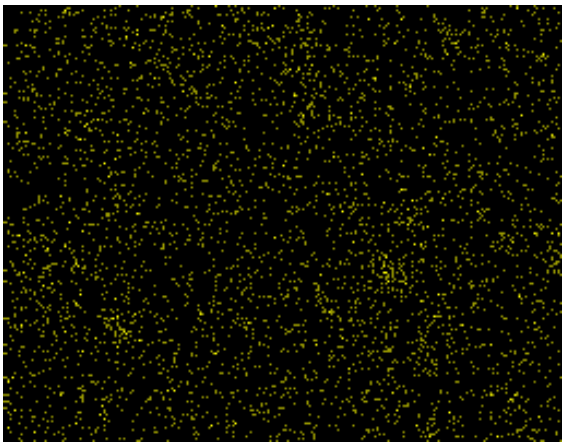

Figure 4.14. EDX mapping of Ru/ δ-Al_2O_3 with 1.04 wt% Ru content (spent catalyst).

SEM micrographs of the reduced fresh and spent catalyst samples are shown in Figures 4.15-4.20. For comparison purposes, analyses are conducted at same magnification of 50000x. Light elements appear dark in contrast whereas heavy elements, specifically the reduced metals such as Pt, Rh and Ru appear as bright spots. Rh sites are difficult to visualize but their dispersions on both fresh and spent catalysts are similar as observed in mapping results. Ru sites seem to be dispersed more uniformly than Rh, but the dispersion patterns in the EDX maps give better results for the Rh catalyst (Figures 4.11 and 4.13, Figures 4.12 and 4.14). Dispersion of Pt sites are found to be better on both SEM micrographs (Figures 4.15 and 4.16) and EDX maps (Figures 4.9 and 4.10).

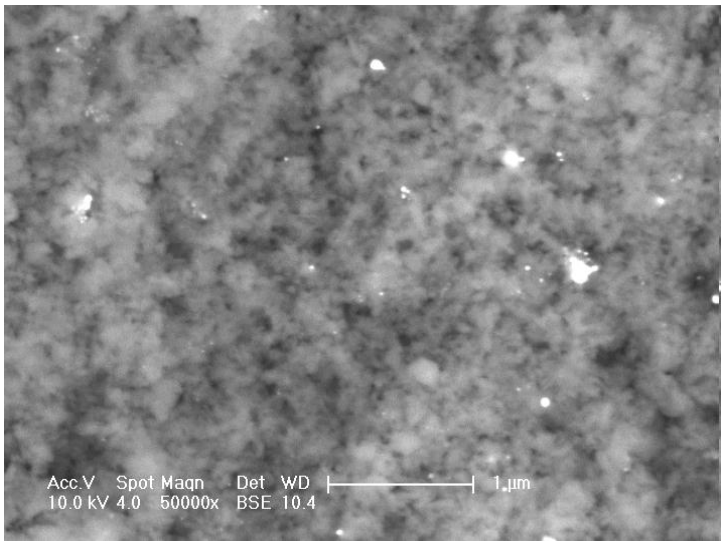

Figure 4.15. SEM image of Pt/ δ-Al_2O_3 with 1.85 wt% Pt content (fresh catalyst).

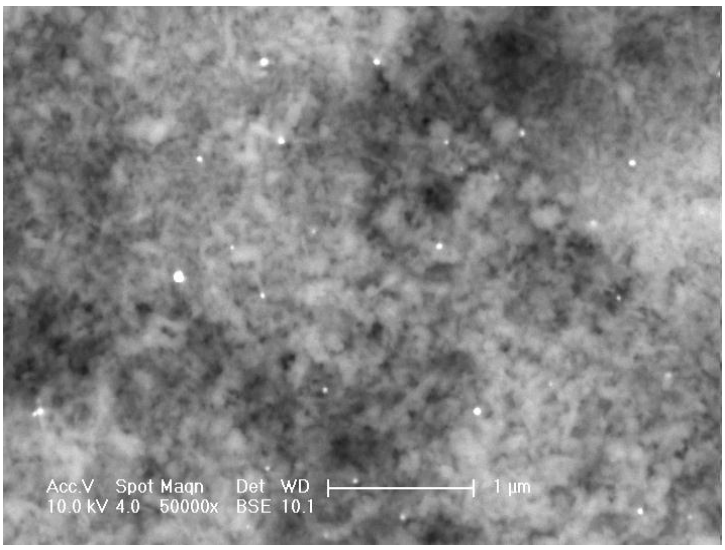

Figure 4.16. SEM image of Pt/ δ-Al_2O_3 with 1.69 wt% Pt content (spent catalyst).

Spent catalyst on every coated plate is post-characterized under SEM for potential coke formation. Figure 4.16, 4.18 and 4.20 shows the micrographs of the spent Pt, Rh and Ru-based catalysts on the plates used in oxidation experiments run with 100 ml/min feed flow at different CH_4/O_2 ratios. Carbonaceous deposits are not detected over either catalyst.

Moreover, no significant weight loss is detected after the reactions. This shows that the catalyst coatings remain mechanically stable in the course of the experiments and verify the validity of the coating method employed in this study.

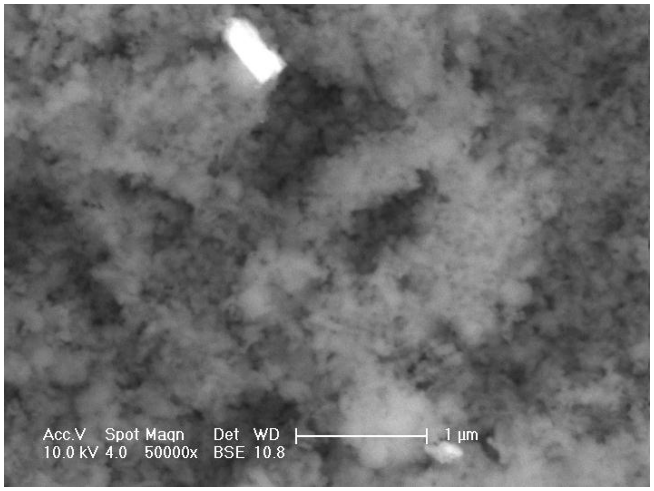

Figure 4.17. SEM image of Rh/ δ-Al_2O_3 with 2.19 wt% Rh content (fresh catalyst).

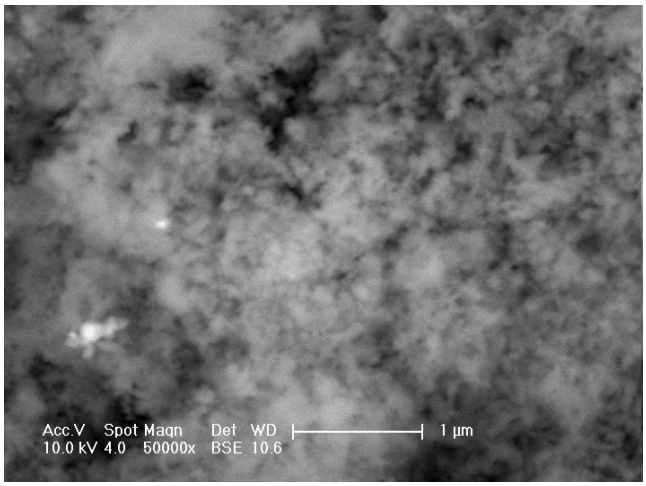

Figure 4.18. SEM image of Rh/ δ-Al_2O_3 with 2.34 wt% Rh content (spent catalyst).

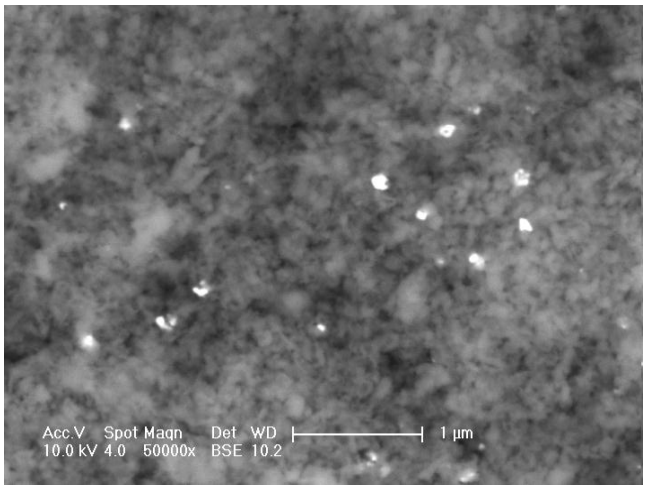

Figure 4.19. SEM image of Ru/ δ-Al_2O_3 with 1.85 wt% Ru content (fresh catalyst).

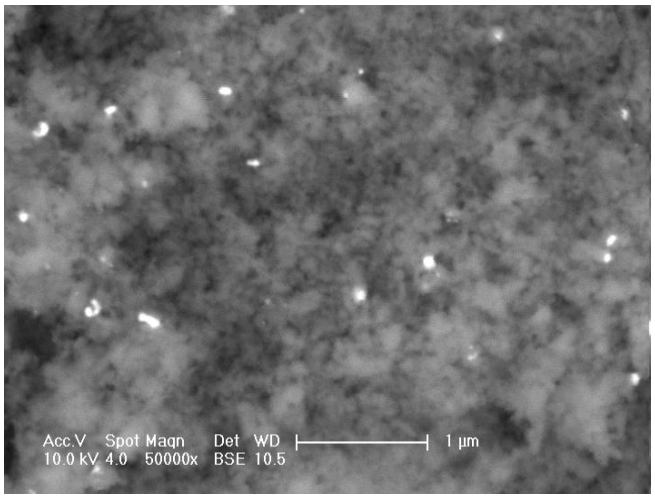

Figure 4.20. SEM image of Ru/ δ-Al_2O_3 with 1.04 wt% Ru content (spent catalyst).

5. CONCLUSIONS

Methane oxidation activity of 2 wt% Pt/δ-Al_2O_3, 2 wt% Rh/δ-Al_2O_3 and 2 wt% Ru/δ-Al_2O_3 coated microchannels are investigated under fuel rich conditions. Catalyst activity is expressed in terms of methane conversion that is measured at different CH_4/O_2 feed ratios and at different total feed flow rates with respect to increasing temperature. Catalysts are compared on the basis of their light-off temperature, which is defined as the value at which 10% of methane conversion is achieved. Catalyst activity is found to follow the order of Pt/δ-Al_2O_3 > Rh/δ-Al_2O_3 > Ru/δ-Al_2O_3 with respect to their light-off temperature. When the CH_4/O_2 ratio is increased, light-off temperatures are found to decrease to a certain value then start to increase again for all catalysts. The formation of minimum light-off temperatures is observed to be at CH_4/O_2 ratios of 1.6 for Pt/δ-Al_2O_3 and Rh/δ-Al_2O_3, and 1.82 for Ru/γ-Al_2O_3. Catalytic activity tests are also conducted by changing the total feed flow rate (75, 100 and 125 ml/min) at constant CH_4/O_2 ratio of 1.85. Methane conversions over Pt and Ru are found to be the highest at 75 ml/min flow, whereas highest conversions over Rh are obtained at 100 ml/min. At 75 ml/min, the increased contact of reactive flow with the Pt and Ru catalysts led to increased methane conversions. The different response of Rh against flow rate is attributed to its high catalytic activity that is capable of delivering high conversions despite reduced contact time. SEM and EDX analyses conducted over reduced fresh and spent catalysts samples show that the targeted metal content is successfully coated to the microchannels and Pt and Rh metals are dispersed uniformly over the support. However, some agglomeration is detected for Ru, which is a possible reason for its low catalytic activity. No coke formation occurred even the catalysts are operated under fuel rich conditions and at high temperatures. Catalyst coatings remained mechanically stable during the experiments.

6. RECOMMENDATIONS

Following recommendations can be used to improve the thesis study:

- Catalyst loadings on support kept constant at 2 wt% during experimental study. Catalyst activity could be compared according to different amounts of metal loading.

- Instead of stainless steel reactor, quartz tube reactor could be used. Quartz tube reactor can resists higher temperatures. Also fitting operation of housing material into the reactor can be observed through transparent structure of quartz reactor. As a result bypass risk can be minimized.

- Microchannel reactor could be compared with packed bed reactor in terms of productivity and performance.

APPENDIX A: MASS FLOW CONTROL CALIBRATION

Calibration curves of the mass flow controllers used in the experiments are illustrated below.

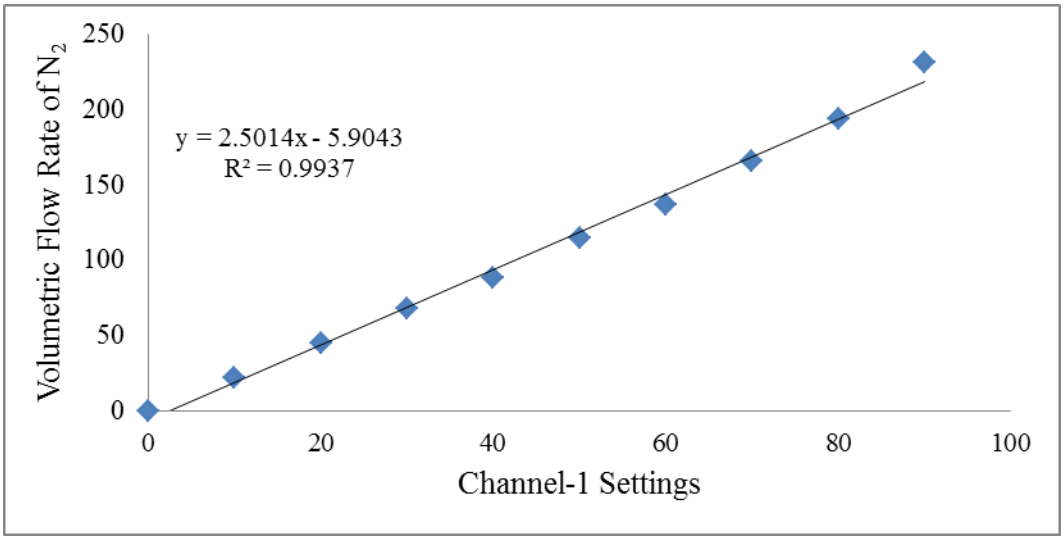

Figure A.1. Calibration curve of the methane mass flow controller.

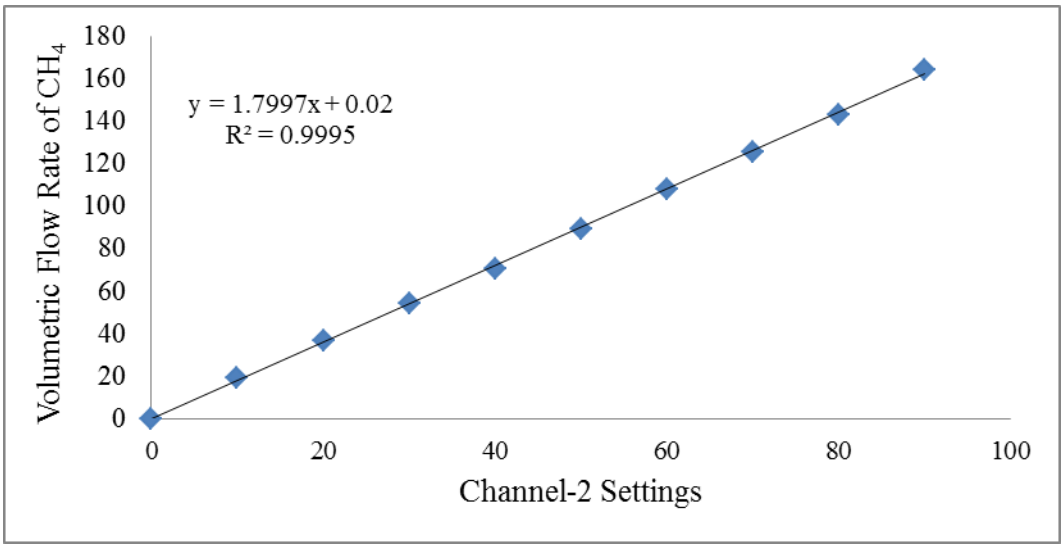

Figure A.2. Calibration curve of the nitrogen mass flow controller.

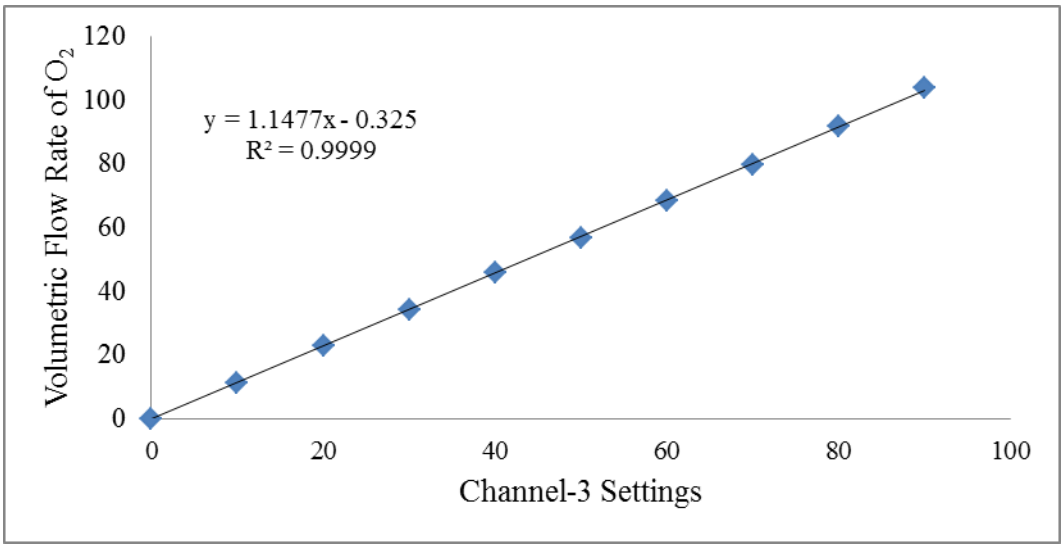

Figure A.3. Calibration curve of the oxygen mass flow controller.

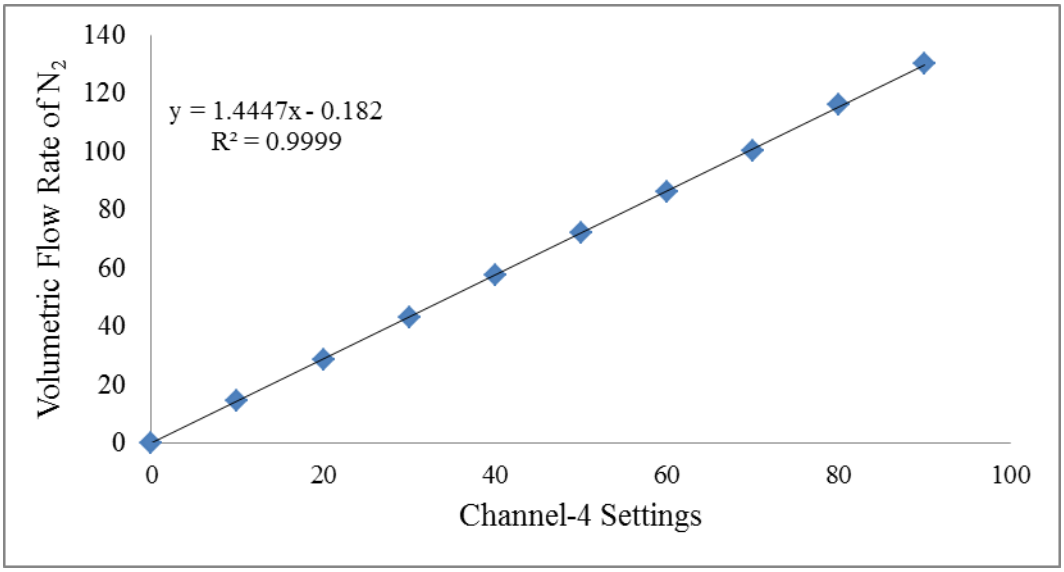

Figure A.4. Calibration curve of the hydrogen mass flow controller.

APPENDIX B: GAS CHROMOTOGRAPH CALIBRATION

Calibration curves of the gas chromatograph used in the experiments are given below.

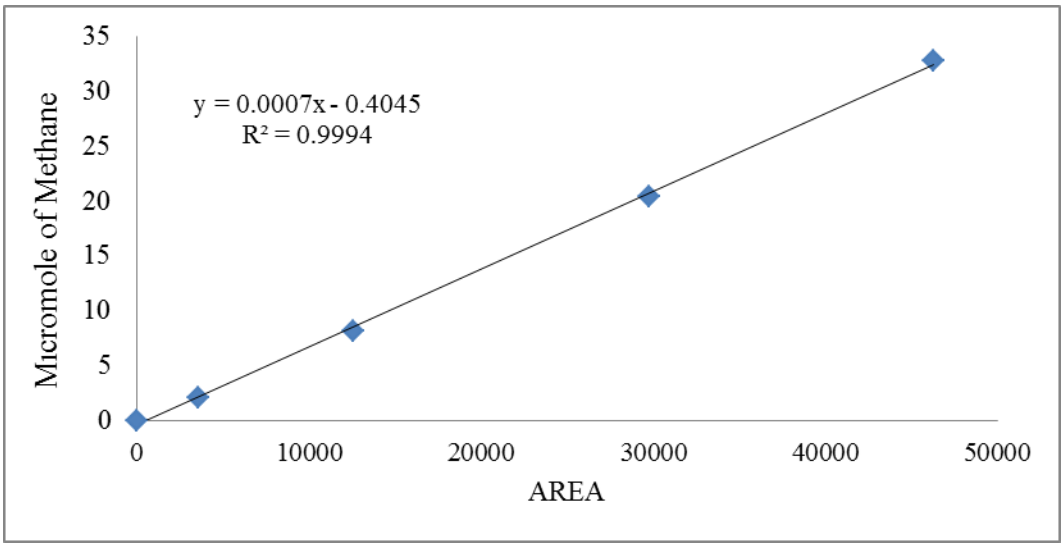

Figure B.1. Calibration curve of methane

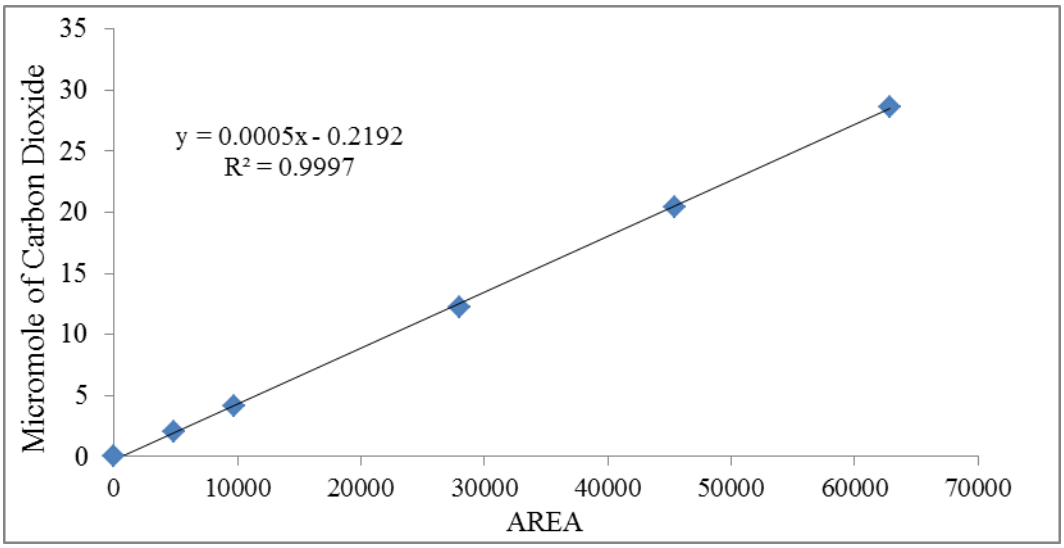

Figure B.2. Calibration curve of carbon dioxide

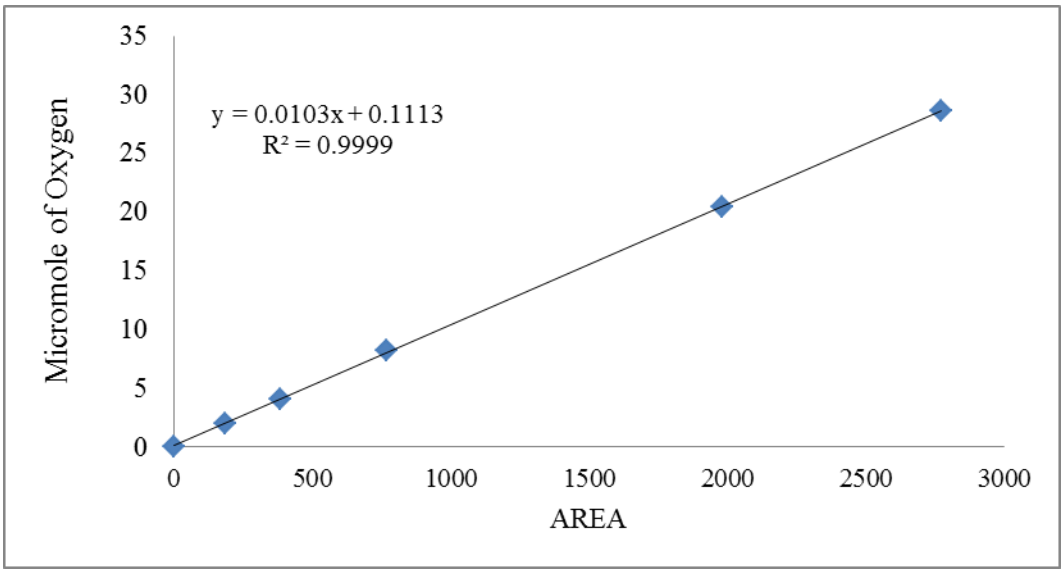

Figure B.3. Calibration curve of oxygen

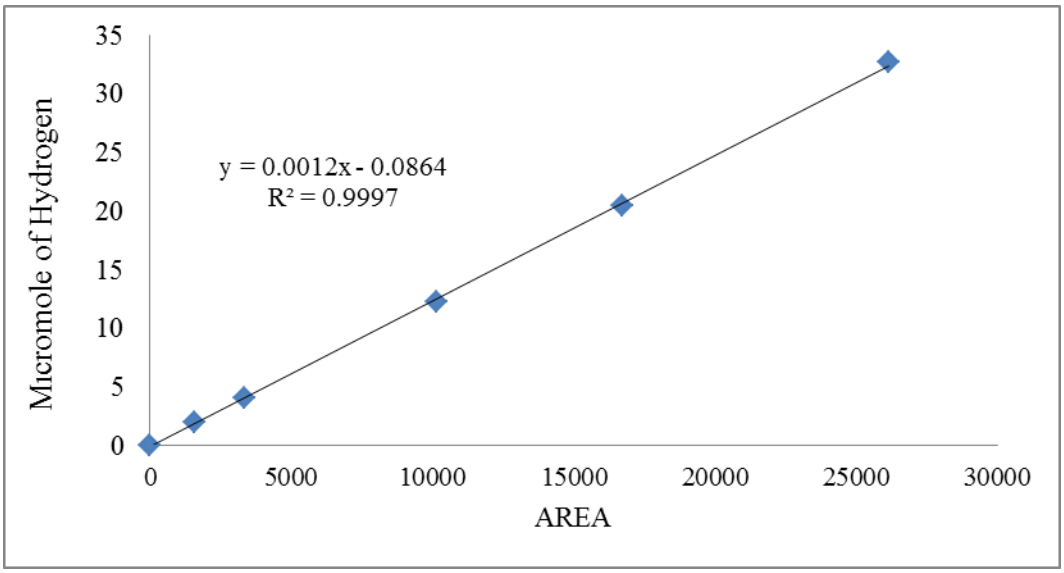

Figure B.4. Calibration curve of hydrogen

REFERENCES

Avcı, A. K., D. L. Trimm, and M. Karakaya, "Microreactor Catalytic Combustion for Chemicals Processing", *Catalysis Today,* Vol. 155, pp. 66-74, 2010.

Avcı A.K., D. L. Trimm, A. E. Aksoylu, and Z. I. Onsan, "Hydrogen Production by Steam Reforming of N-butane over Supported Ni and Pt-Ni Catalysts", *Applied Catalyst A, Vol.* 258, pp. 235–240, 2004.

Avcı, A. K., D. L. Trimm, A. E. Aksoylu, and Z. I. Onsan, "Ignition Characteristics of Pt, Ni and Pt–Ni Catalysts Used for Autothermal Fuel Processing", *Catalysis Letters,* Vol. 88, No. 1-2, 2003.

Bounechada, D., G. Groppi, P. Forzatti, K. Kallinen, and T. Kinnunen, "Effect of Periodic lean/rich Switch on Methane Conversion over a Ce-Zr Promoted Pd-Rh/Al2O3 Catalyst in the Exhausts of Natural Gas Vehicles", *Applied Catalysis B: Environmental*, Vol. 119-120, pp. 91–99, 2012.

Brabbs, T.A., and S.A. Merritt, "Fuel-rich Catalytic Combustion of a High Density Fuel", *NASA Technical Paper 3281*, 1993.

Burch, R., and P.K. Loader, "Investigation of Pt/Al_2O_3 and Pd/Al_2O_3 Catalysts for the Combustion of Methane at Low Concentrations", *Applied Catalysis B, Environmental*, Vol. 5, pp. 149–164, 1994.

Carlsson, P., E. Fridell, and M. Skoglundh, "Methane Oxidation over Pt/Al_2O_3 and Pd/Al_2O_3 Catalysts under Transient Conditions", *Catalysis Letters,* Vol. 115, pp. 1–2, 2007.

Charpentier, J. C., "In the Frame of Globalization and Sustainability, Process Intensification, a Path to the Future of Chemical and Process Engineering (Molecules into Money)", *Chemical Engineering Journal*, Vol. 134, pp. 84–92, 2007.

Da Silva, M. A. P., and M. Schmal, "Reduction of NO by CO on Pt-MoO_3/γ-Al_2O_3 catalysts", *Catalysis Today*, Vol. 85, pp. 31–37, 2003.

Ehrfeld, W., V. Hessel, and H. Lowe, *Microreactors: New Technology for Modern Chemistry*, Wiley-VCH Verlag GmbH, Weinheim, Germany, 2000.

Eriksson, S., M. Wolf, A. Schneider, J. Mantzaras, F. Raimondi, M. Boutonnet, and S. Ja¨ra, "Fuel-Rich Catalytic Combustion of Methane in Zero Emissions Power Generation Processes", *Catalysis Today*, Vol. 117, pp. 447–453, 2006.

Fichtner, M., J. Mayer, D. Wolf, and K. Schubert, "Microstructured Rhodium Catalysts for the Partial Oxidation of Methane to Syngas under Pressure", *Industrial & Engineering Chemistry Research*, Vol. 40, pp. 3475–3483, 2001.

Gandia, L.M., G. Arzamendi, P.M. Dieguez, M. Montes, J.A. Odriozola, and E. Falabella Sousa-Aguiar, "Methane Steam Reforming in a Microchannel Reactor for GTL Intensification: A Computational Fluid Dynamics Simulation Study", *Chemical Engineering Journal*, Vol. 154, pp. 168–173, 2009.

Guan, G., K. Kusakabe, M. Taneda, M. Uehara, and H. Maeda, "Catalytic Combustion of Methane over Pd-based Catalyst Supported on a Macroporous Alumina Layer in a Microchannel Reactor", *Chemical Engineering Journal*, Vol. 144, pp. 270–276, 2008.

Hessel, V., and G. Kolb, "Microstructured Reactors for Gas Phase Reactions", *Chemical Engineering Journal*, Vol. 98, pp. 1–38, 2004.

Hickman, D. A., E. A. Haupfear, and L. D. Schmidt, "Synthesis Gas Formation by Direct Oxidation of Methane over Rh Monoliths", *CATALYSIS LETTERS*, Vol. 17, p.223, 1993.

Jiang, Z., J. Yu, J. Cheng, T. Xiao, M. O. Jones, Z. Hao, and P. P. Edwards, "Catalytic Combustion of Methane over Mixed Oxides Derived from Co-Mg/Al Ternary Hydrotalcites", *Fuel Processing Technology*, Vol. 91, pp. 97–102, 2010.

Jiang, Z., W. Huang, H. Zhao, Z. Zhang, D. Tan, and X. Bao, "Dispersion and Site-blocking Effect of Molybdenum Oxide for CO Chemisorption on the Pt(1 1 0) Substrate", *Journal of Molecular Catalysis A: Chemical*, Vol. 268, pp. 213–220, 2007.

Karakaya, M., S. Keskin, and A. K. Avcı, "Parametric Study of Methane Steam Reforming to Syngas in a Catalytic Microchannel Reactor", *Applied Catalysis A: General,* Vol. 411–412, pp. 114–122, 2012.

Lerou, J.J., A.L. Tonkovich, L. Silva, S. Perry, and J. McDaniel, "Microchannel Reactor Architecture Enables Greener Processes", *Chemical Engineering Science,* Vol. 65, pp. 380–385, 2010.

Lyubovsky, M., L. L.Smith, M. Castaldi, H. Karim, B. Nentwick, S. Etemad, R. LaPierre, and W. C. Pfefferle, "Catalytic Combustion over Platinum Group Catalysts: Fuel-lean versus Fuel-rich Operation", *Catalysis Today*, Vol. 83, pp. 71–84, 2003.

Mallens, E. P. J., J. H. B. J. Hoebink, and G. B. Marin, The Reaction Mechanism of the Partial Oxidation of Methane to Synthesis Gas: A Transient Kinetic Study over Rhodium and a Comparison with Platinum, *Journal of Catalysis*, Vol. 167, pp.43–56, 1997.

O'Connell, M., G. Kolb, R. Zapf, Y. Mena, and V. Hessel, "Bimetallic Catalysts for the Catalytic Combustion of Methane Using Microreactor Technology", *Catalysis Today*, Vol. 144, pp. 306–311, 2009.

Persson, K., K. Jansson, and S. G. Järås, "Characterization and Microstructure of Pd and Bimetallic Pd-Pt Catalysts during Methane Oxidation", *Journal of Catalysis*, Vol. 245, pp. 401–414, 2007.

Renken, A., and L. Kiwi-Minsker, "Microstructured Reactors for Catalytic Reactions", *Catalysis Today*, Vol.110, pp. 2–14, 2005.

Rollbuhler, R.J., "Proceedings of the 27th Joint Propulsion Conference, Sacramento, CA", *NASA Technical Memorandum 104423,* AIAA Paper No. 91–2463, 1991.

Seris, E.L.C., G. Abramowitz, A. M. Johnston, and B. S. Haynes, "Scaleable, Microstructured Plant for Steam Reforming of Methane", *Chemical Engineering Journal*, Vol.135, pp. 9–16, 2008.

Şen, Ö., *Constructing and Testing of a Low-Temperature Water-Gas Shift Reaction System*, M. S. Thesis, Boğaziçi University, Istanbul, 2008.

Tonkovich, A.Y., S. Perry, Y. Wang, D. Qui, T. LaPlante, and W.A. Rogers, "Microchannel Process Technology for Compact Methane Steam Reforming", *Chemical Engineering Science*, Vol. 59, pp. 4819–4824, 2004.

Veser, G., and J. Frauhammer, "Modelling Steady State and Ignition During Catalytic Methane Oxidation in a Monolith Reactor", *Chemical Engineering Science*, Vol. 55, pp. 2271–2286, 2000.

Wang, H.Y., and E. Ruckenstein, "Catalytic Partial Oxidation of Methane to Synthesis Gas over Al_2O_3 Supported Rhodium Catalysts", *Catalysis Letters*, Vol. 59, pp. 121–127, 1999.

Wierzb, I., and A. Depiak, 2003, "The Catalytic Oxidation of Heated Lean Homogeneously Premixed Gaseous Fuel Air Streams", *Chemical Engineering Journal*, Vol. 91, pp. 287–294, 2003.

Wirth, T., *Microreactors in Organic Synthesis and Catalysis*, Wiley-VCH Verlag GmbH, Weinheim, Germany, 2008.